J. Fluid Mech. (1993), *vol.* 253, *pp.* 67–103

Nonlinear stability of combustion-driven acoustic oscillations in resonance tubes

By STEPHEN B. MARGOLIS
Combustion Research Facility, Sandia National Laboratories, Livermore, CA 94551, USA

(Received 27 March 1992 and in revised form 29 January 1993)

The leading-order fluid motions and frequencies in resonance tubes coupled to a combustion-driven flow source, such as occurs in various types of pulse combustors, are usually strongly related to those predicted by linear acoustics. However, in order to determine the amplitudes of the infinite number of classical acoustic modes predicted by linear theory alone, and hence the complete solution, a nonlinear analysis is required. In the present work, we adopt a formal perturbation approach based on the smallness of the mean-flow Mach number which, as a consequence of solvability conditions at higher orders in the analysis, results in an infinitely coupled system of nonlinear evolution equations for the amplitudes of the linear acoustic modes. An analysis of these amplitude equations then shows that the combination of driving processes, such as combustion, that supply energy to the acoustic oscillations and those, such as viscous effects, that dampen such motions, in conjunction with the manner in which the resonance tube is coupled to its flow source, provides an effective mode-selection mechanism that inhibits the (linear) growth of all but a few of the lower-frequency modes. For the common case of long resonance tubes, the lowest frequencies correspond to purely longitudinal modes, and we analyse in detail the solution behaviour for a typical situation in which only the first of these has a positive linear growth rate. Basic truncation strategies for the infinitely coupled amplitudes are discussed, and we demonstrate, based on analyses with both two and three modes, the stable bifurcation of an acoustic oscillation, or limit cycle, at a critical value of an appropriate bifurcation parameter. In addition, we show that the bifurcated solution branch has a turning point at a second critical value of the bifurcation parameter beyond which no stable bounded solutions exist.

1. Introduction

The subject of combustion-driven acoustic oscillations is of fundamental importance in a number of practical combustor applications. Notable examples include propulsion systems such as solid and liquid rocket motors, and modern pulse combustors such as those used for heating and drying applications. In the case of rocket motors, such acoustic oscillations are commonplace and are generally referred to as combustion instabilities.† As the term 'instability' in a practical context often implies, they are primarily important in propulsion because large-amplitude oscillations can lead to unacceptable structural vibrations and even failure. In the case of pulse combustors, on

† This terminology is, unfortunately, rather ambiguous, since there exist other well-known types of non-acoustic instabilities in propellant combustion that arise owing to both hydrodynamic and double-diffusive ('diffusional/thermal') effects (cf. Williams 1985; Margolis & Williams 1988, 1989; Bechtold & Margolis 1989, 1991).

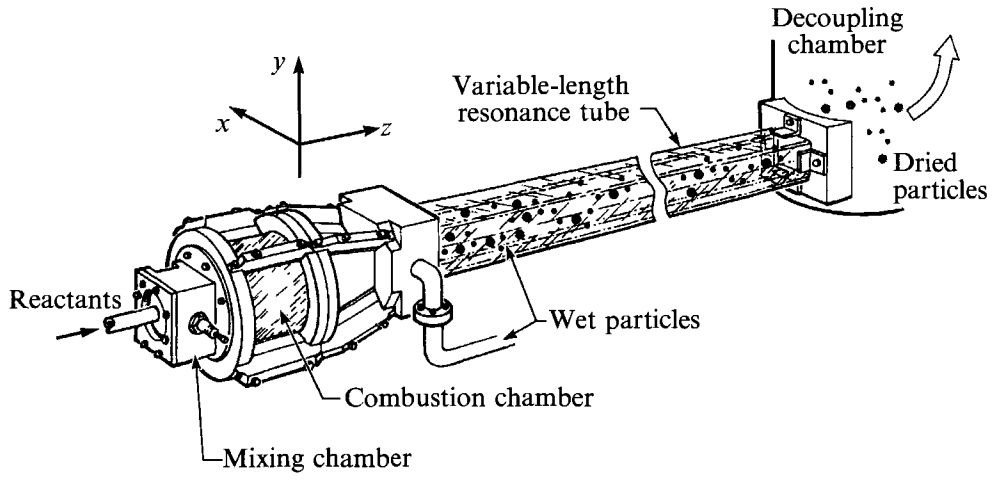

FIGURE 1. Geometry of the model pulse combustor considered here. Particles are injected at the entrance to the resonance tube, which is fed by the flow from the combustion chamber.

the other hand, the oscillations are favourable from the standpoint of efficiency, since pulse combustors can be self-pumping and lead to enhanced rates of heat transfer and/or evaporation. Here too, however, large oscillation amplitudes are often unacceptable owing not only to accompanying noise levels, but also for the same reasons that apply to rocket motors. Indeed, one of the earliest and most well-known applications of the pulse combustor was its use to propel the V-1 buzz-bomb in World War II (cf. Putnam, Belles & Kentfield 1986).

Whether one is talking about acoustic oscillations in the resonance tube of a pulse combustor (see figure 1) or acoustic oscillations in a rocket chamber, the fundamental problem is similar in that one wishes to study the nature of acoustic oscillations in a partially enclosed volume as a function of various parameters. Although these oscillations are intrinsic to the geometry of the volume (indeed, the equations of linear acoustics typically emerge in a first approximation), they are, in fact, also driven by the energy released due to the occurrence of combustion in some part of the system. Hence, such oscillations are said to be combustion-driven, and it is this coupling to the combustion processes that distinguishes such problems from other branches of acoustics. Though the details of the analysis differ for the above two types of combustion-driven problems (owing primarily to differences in the boundary conditions, as discussed below), it is nonetheless true that in both problems classical acoustic modes in the chamber/resonance tube play a primarily role, and consequently, the same general type of analysis is applicable to both problems. Indeed, the type of analysis performed here is relevant to an even wider range of gasdynamic problems that lead to forced acoustic oscillations. For example, the forced motion of a piston in a cylinder also leads to a similar type of acoustic problem, although the more direct driving of the oscillations through the motion of the piston leads to steep waves and shocks that, as a general rule, require much greater modal resolution than the combustion-driven acoustic oscillations considered here (cf. Wang & Kassoy 1990*a–c*).

Thus, although the focus in this work is on the resonance tube/pulse combustor application as discussed below, the approach that we have adopted in the present work, as well as in a preliminary study (Margolis 1992), is closely related to the methods that have been developed for treating acoustic instabilities in solid and liquid propellant

rocket motors (cf. Culick 1976*a*, *b*, 1990; Culick & Yang 1992). As in the propellant work, we obtain the classical equations of linear acoustics as the leading-order perturbation to the basic flow in the resonance tube, with effects due to coupling with the combustion chamber and other processes within the resonance tube appearing as higher-order perturbations. The challenge is then to determine the amplitudes of the infinite number of classical acoustic modes that are present as a function of the parameters in the problem. In the rocket motor problem, the adopted procedure has been to reduce the problem to a set of ordinary differential equations for the time-dependent amplitudes via a form of spatial averaging based on Galerkin's method, followed by either direct numerical integration of the amplitude equations (Zinn & Powell 1970) or by time-averaging (Culick 1976*a*, *b*). In the present problem, however, we have introduced an alternative, more formal approach based on nonlinear stability theory (cf. Matkowsky 1970; Margolis & Matkowsky 1983). In particular, we have constructed a formal perturbation procedure that provides infinitely coupled first-order evolution equations for the amplitudes of the linear acoustic modes as a consequence of appropriate solvability conditions at higher orders in the analysis. The linearized form of these equations then determines conditions for the (linear) growth or decay of individual acoustic modes, while an analysis of an appropriately truncated subset of the full nonlinear system describes the long-time dynamics of the acoustic oscillations.

As indicated above, we here apply the approach just described to a model of a Helmholtz-type pulse combustor introduced in our preliminary work (Margolis 1992) and illustrated in figure 1. We have chosen this application partly because it is a new application for this type of analysis, and partly because the difference in boundary conditions results in a completely different set of amplitude equations. In particular, the resulting evolution equations for the acoustic amplitudes contain cubic nonlinearities, rather than the quadratic nonlinearities that are obtained for the propellant-type problems (Culick 1976*a*, *b*). In this model, as in other possible models of pulse combustors, there is a periodic flow field associated with acoustic instabilities in a resonance tube, which in turn is coupled in some fashion to a combustion chamber that supplies energy to the acoustic field. Consequently, owing to various damping effects within and/or on the boundaries of the resonance tube, initially infinitesimal perturbations may either decay or grow to some finite amplitude. In the latter case, the resulting oscillating flow field may offer distinct advantages over one that is steady in a wide variety of applications (cf. Putnam *et al.* 1986; Barr *et al.* 1988, 1990; Dec & Keller 1990; Dec, Keller & Hongo 1991; Bramlette & Keller 1987). The specific problem modelled here is that of a pulse combustor used in moisture removal, or drying, applications. A combustion chamber is attached to a resonance tube, and wet particles are injected at or very near the entrance to the latter, which in turn is attached to a larger decoupling chamber in which an essentially constant pressure is maintained. The advantage of using a pulse combustor for such purposes lies in the fact that the oscillating flow field usually enhances drying efficiency (Bramlette & Keller 1987), but in the present context, it serves primarily as a convenient, yet physical, model for illustrating a general approach to analysing acoustic instabilities in partially enclosed volumes.

In what follows, we first summarize the mathematical model of the pulse combustor described above. We then introduce appropriate scalings and show how the magnitude of the acoustic perturbation amplitude can be formally related to the mean-flow Mach number in the typical case when the latter is small. This allows a perturbation expansion of all variables in appropriate powers of a single small quantity, and enables

us to formally derive the equations for linear acoustics governing the leading-order perturbation from steady, one-dimensional flow through the resonance tube. The sequence of problems that emerge at higher orders in the analysis are then inhomogeneous versions of the leading-order problem, solvability conditions for which lead to infinitely coupled nonlinear evolution equations for the amplitudes of the classical acoustic modes predicted by the leading-order analysis. A linearization of these equations then allows the determination of the growth or decay rate of each modal component of an infinitesimal acoustic perturbation as a function of the various parameters in the problem. This information in turn serves as a guide in the formulation of appropriate truncation schemes for the full, infinitely coupled, nonlinear system. These results are illustrated for a typical situation in which the lowest-frequency mode has a positive linear growth rate, while the remaining modes all decay according to the linearized amplitude equations. Using both two- and three-mode truncations of the full nonlinear evolution equations, we then construct the bifurcation diagram for the amplitude of an acoustic oscillation, or limit cycle, as a function of a parameter that measures the strength of the coupling between velocity and pressure at the entrance to the resonance tube.

2. The mathematical model

The model for the pulse combustor introduced in a recent preliminary study (Margolis 1992) and depicted in figure 1 consists of appropriate conservation equations for two-phase flow within the resonance tube, subject to certain conditions at the entrance and exit of the tube, as well as boundary conditions on the sidewalls. As we shall show, it turns out that the only essential requirement for the maintenance of a time-dependent flow field associated with acoustic instabilities is that there be a dynamic balance between processes that supply energy to the acoustic motions, and those that act to dampen such motions. Accordingly, we shall deliberately keep the model as simple as possible in order to capture only the most essential features for obtaining the amplitude equations that govern the bifurcation of an acoustic oscillation. In particular, we circumvent the complex details of the combustion/acoustic interactions by representing them in the form of a phenomenological coupling between the velocity and pressure fields at the entrance to the resonance tube. We also consider only the limiting (equilibrium) case of infinitesimally small particles so that velocity and temperature differences between the gas and the particles are negligible. Thus, coupling of the gas and particle phases occurs solely due to evaporation from the initially wet particles, which, along with certain viscous effects, constitute the only potential damping mechanisms within the resonance tube itself. However, virtually all processes that may assume quantitative importance may, if desired, be treated explicitly within the general context of the present analysis. The present model, on the other hand, is sufficient to illustrate the general approach and to give the essential physical results regarding the nonlinear stability of acoustic oscillations.

2.1. *Governing equations*

Under the above assumptions, the governing equations within the tube reduce to conservation of particle density ($\tilde{\rho}_\pi$),

$$\frac{\partial \tilde{\rho}_\pi}{\partial \tilde{t}} + \tilde{\nabla} \cdot (\tilde{\rho}_\pi \tilde{\boldsymbol{u}}) = \tilde{r}(\tilde{p}, \tilde{T}); \tag{2.1}$$

conservation of gas density ($\tilde{\rho}_g$), which, when combined with that for particle density, gives the overall mass conservation equation for the total density ($\tilde{\rho}$),

$$\frac{\partial \tilde{\rho}}{\partial \tilde{t}} + \tilde{\nabla} \cdot (\tilde{\rho} \tilde{\boldsymbol{u}}) = 0; \tag{2.2}$$

conservation of total momentum ($\tilde{\rho}\tilde{\boldsymbol{u}}$),

$$\tilde{\rho} \frac{\partial \tilde{\boldsymbol{u}}}{\partial \tilde{t}} + \tilde{\rho}(\tilde{\boldsymbol{u}} \cdot \tilde{\nabla}) \tilde{\boldsymbol{u}} = -\tilde{\nabla} \tilde{p} + \tilde{\mu} \tilde{\nabla}^2 \tilde{\boldsymbol{u}} + \tfrac{1}{3} \tilde{\mu} \tilde{\nabla} (\tilde{\nabla} \cdot \tilde{\boldsymbol{u}}); \tag{2.3}$$

and conservation of energy. The last, when combined with the gas-phase equation of state $\tilde{p} = \tilde{\rho}_g \tilde{R} \tilde{T} = (\tilde{\rho} - \tilde{\rho}_\pi) \tilde{R} \tilde{T}$, which is equivalent to the average equation of state

$$\tilde{p} = \tilde{\rho} \bar{R} \tilde{T}, \quad \bar{R} \equiv (1 - \tilde{\rho}_\pi / \tilde{\rho}) \tilde{R} \tag{2.4}$$

for the two-phase flow (cf. Marble 1970), can be put in the form of an equation for pressure ($\tilde{p}$) according to

$$\frac{\partial \tilde{p}}{\partial \tilde{t}} + \tilde{\boldsymbol{u}} \cdot \tilde{\nabla} \tilde{p} + \bar{\gamma} \tilde{p} \tilde{\nabla} \cdot \tilde{\boldsymbol{u}} = \tilde{p} \left(\frac{\partial \ln \bar{R}}{\partial \tilde{t}} + \tilde{\boldsymbol{u}} \cdot \tilde{\nabla} \ln \bar{R} \right) + (\bar{\gamma} - 1)[\tilde{L} \tilde{r}(\tilde{p}, \tilde{T}) + \tilde{\mu} \tilde{\Phi}]. \tag{2.5}$$

Here, $\tilde{R}$ is the gas constant, $\tilde{\mu}$ is the coefficient of viscosity (assumed constant), $\tilde{\mu}\tilde{\Phi}$ is the viscous dissipation, $\tilde{r} < 0$ is the vaporization rate, and $\tilde{L} > 0$ is the heat of vaporization. For simplicity, thermal diffusion has been neglected, so in essence we are considering the case of an infinite-Prandtl-number fluid. In addition, we have introduced the ratio of average specific heats $\bar{\gamma} \equiv \bar{c}_p / \bar{c}_v$ and the effective gas constant $\bar{R} \equiv \bar{c}_p / \bar{c}_v$ (in contrast to their gas-phase counterparts $\gamma = \tilde{c}_p / \tilde{c}_v$ and $\tilde{R} = \tilde{c}_p - \tilde{c}_v$), where $\bar{c}_p$ and $\bar{c}_v$ are defined in terms of the single-phase heat capacities $\tilde{c}_p$, $\tilde{c}_v$ (gas) and $\tilde{c}_\pi$ (particles) by

$$\bar{c}_p = (1 - \tilde{\rho}_\pi / \tilde{\rho}) \tilde{c}_p + (\tilde{\rho}_\pi / \tilde{\rho}) \tilde{c}_\pi, \quad \bar{c}_v = (1 - \tilde{\rho}_\pi / \tilde{\rho}) \tilde{c}_v + (\tilde{\rho}_\pi / \tilde{\rho}) \tilde{c}_\pi.$$

We note that the particle density varies not only owing to kinematics, but also owing to vaporization from the wet particles, which is accounted for by the negative production term in the particle mass and total energy equations. Thus, the particle density $\tilde{\rho}_\pi = \tilde{\rho}_\sigma + \tilde{\rho}_\lambda$, where $\tilde{\rho}_\sigma$ and $\tilde{\rho}_\lambda$ are the solid inert and vaporizable liquid components, respectively, of the total particle density $\tilde{\rho}_\pi$. The dependence of the vaporization rate $\tilde{r}$ on pressure and temperature is safely assumed to be such that $\partial |\tilde{r}| / \partial \tilde{T} > 0$ and $\partial |\tilde{r}| / \partial \tilde{p} < 0$, but may otherwise be empirically correlated with actual data or modelled according to various droplet and spray vaporization considerations (cf. Prakash & Sirignano 1980; Law 1982; Williams 1985). In the present work, however, the scale of the particle loading will be sufficiently small (see below) so that the local pressure and temperature dependence of $\tilde{r}$ will not enter into our analysis through the order needed to obtain evolution equations for the leading-order acoustic oscillations.

To complete the specification of the problem, we prescribe the boundary conditions

$$\tilde{p}|_{\tilde{z} = \tilde{H}} = \tilde{p}_0, \quad \boldsymbol{n} \cdot \tilde{\boldsymbol{u}}|_C = 0, \quad \tilde{\boldsymbol{u}}|_{\tilde{z}=0} = \{0, 0, \tilde{f}[\tilde{p}(\tilde{t} - \tilde{t}_d)]\}, \tag{2.6a–c}$$

corresponding to an imposed pressure at the exit of the resonance tube, no mass penetration at the sidewalls C, and a functional relationship between pressure and the inflow velocity at the entrance to the resonance tube. In Appendix B, we show how these conditions may be modified, using admittance/impedance conditions similar to (2.6*c*), to explicitly treat additional boundary effects associated with acoustic damping

at the sidewalls owing to a viscous boundary layer and radiation damping out the end of the resonance tube. For the present, however, we suppress the formal consideration of these effects, thereby eliminating the need for a no-slip constraint on the velocity components and ultimately giving a pressure node condition at the exit. Furthermore, it turns out (Appendix B) that the various types of damping processes that arise in this problem all lead to the same form of the amplitude equations that determine the acoustic bifurcation discussed in §§6 and 7. Consequently, we may now regard the viscosity coefficient $\tilde{\mu}$ as a phenomenological parameter that accounts in some qualitative sense for all damping phenomena in the problem. We also note that the neglect of thermal diffusion relative to the empirically larger viscous diffusion term in (2.3) precludes a specification of a sidewall boundary condition on the temperature. However, it implies that, to a first approximation, we are restricting consideration to the case of adiabatic sidewalls, as can be seen from the fact that the leading-order normal heat flux is zero there (see (3.2) and (3.5*b*) below).

The pressure/velocity relationship (2.6*c*), though also phenomenological in nature, has the advantage of allowing the detailed analysis to be confined to the resonance tube itself, as in the case of the simpler Schmidt tube (cf. Putnam *et al.* 1986), while still allowing a coupling with those processes in other parts of the pulse combustor. The latter is achieved through the introduction of a time delay $\tilde{t}_{\mathrm{d}}$ that, along with the function $\tilde{f}(\tilde{p})$ itself, can be empirically related to the problem geometry and the details of the injection and chemical processes within the combustion chamber, which is here regarded as an adiabatic well-stirred reactor. Although the introduction of a time delay, or lag (Grad 1949; Summerfield 1951), has been criticized for its empiricism in the context of its use in the modelling of rocket motors, the physical separation of the combustion and resonance chambers in the present problem makes it possible to more readily regard such a quantity as a physically controllable parameter. Finally, we remark that the exit condition (2.6*a*), which constitutes a neglect of radiation damping as indicated above, and which is the appropriate limiting case for the pulse combustor problem depicted in figure 1, turns out to give significantly different results from those that are obtained in the corresponding analysis of rocket motor stability, as discussed below. In particular, as long as this condition holds at leading order in the perturbation analysis described here, corresponding to the case in which radiation damping is not a larger effect than other damping processes (Appendix B), it turns out that cubic, rather than quadratic, nonlinearities appear in the equations governing the amplitudes of the classical acoustic modes (§3).

2.2. *Scalings and non-dimensionalizations*

In the absence of particle injection, or loading ($\tilde{\rho}_\pi = 0$), a steady solution of (2.2)–(2.6) is given by the uniform flow state

$$\tilde{p} = \tilde{p}_0, \quad \tilde{\boldsymbol{u}} = (0, 0, \tilde{w}_0), \quad \tilde{T} = \tilde{T}_0, \quad \tilde{\rho} = \tilde{\rho}_0, \tag{2.7}$$

where $\tilde{p}_0$ and $\tilde{\rho}_0$ are related by the gas-phase equation of state $\tilde{p}_0 = \tilde{\rho}_0 \tilde{R} \tilde{T}_0$, $\tilde{T}_0$ is the adiabatic flame temperature in the combustion chamber, and the given velocity $\tilde{w}_0$ is determined by conditions upstream of the combustion chamber. With particle injection, $\tilde{\rho}_{\sigma,0}$, the inert component of the particle density at $z = 0$ for the case of steady flow, is a reference value for the total particle density $\tilde{\rho}_\pi$ (assuming the corresponding liquid component $\tilde{\rho}_{\lambda,0}$ of the steady particle density at $z = 0$ is no larger in magnitude than $\rho_{\sigma,0}$). These quantities may be used to define the reference sound speed $\tilde{a}_0 = (\gamma \tilde{R} \tilde{T}_0)^{\frac{1}{2}}$, which in turn defines the Mach number $M = \tilde{w}_0/\tilde{a}_0$ of the reference steady state (2.7), and a parameter $\delta = \tilde{\rho}_{\sigma,0}/\tilde{\rho}_0$ which measures the size of perturbations due

to particle injection. In what follows, the realistic limit of small M and δ will be exploited to first obtain the steady solution with particle injection, followed by the non-steady equations that govern the behaviour of acoustic perturbations.

Equations (2.7) provide one set of reference values for pressure, velocity, temperature and density. However, it is important to recognize that steady perturbations about this state (owing to the presence of particles) and non-steady acoustic perturbations scale differently in general, since $\tilde{w}_0$ is a characteristic flow velocity for steady perturbations, whereas characteristic velocities associated with acoustic disturbances are simply assumed to be small relative to the sound speed $\tilde{a}_0$, which is used to non-dimensionalize acoustic perturbations. For definiteness, we first introduce non-dimensional quantities that are appropriate for the latter. In particular, we define the non-dimensional coordinates

$$(x, y, z) = (\tilde{x}/\tilde{H}, \tilde{y}/\tilde{H}, \tilde{z}/\tilde{H}), \quad t = \tilde{a}_0 \tilde{t}/\tilde{H}, \tag{2.8}$$

where $\tilde{H}$ is the length of the resonance tube, and the non-dimensional variables

$$p = \tilde{p}/\gamma\tilde{p}_0 = \tilde{p}/\tilde{\rho}_0\tilde{a}_0^2, \quad \boldsymbol{u} = \tilde{\boldsymbol{u}}/\tilde{a}_0, \quad \rho = \tilde{\rho}/\tilde{\rho}_0, \quad \rho_\pi = \tilde{\rho}_\pi/\tilde{\rho}_0 = \delta\hat{\rho}, \quad T = \tilde{T}/\tilde{T}_0. \tag{2.9}$$

On the other hand, alternative non-dimensionalizations for the steady perturbations $\tilde{p}_s$ and $\tilde{\boldsymbol{u}}_s$ of the pressure and velocity fields are

$$p_s = \tilde{p}_s/\tilde{\rho}_0\tilde{w}_0^2 = M^{-2}\tilde{p}_s/\tilde{\rho}_0\tilde{a}_0^2, \quad \boldsymbol{u}_s = \tilde{\boldsymbol{u}}_s/\tilde{w}_0 = M^{-1}\tilde{\boldsymbol{u}}_s/\tilde{a}_0. \tag{2.10}$$

Thus, the steady component of velocity is formally scaled by the (small) Mach number M relative to the non-steady (acoustic) velocity field, and the steady component of the pressure perturbation is scaled by M^2 relative to its non-steady counterpart. In a similar fashion, it is appropriate to non-dimensionalize the particle density $\tilde{\rho}_\pi$ by $\tilde{\rho}_{\sigma,0}$ rather than by $\tilde{\rho}_0$, which accounts for the scaling $\rho_\pi = \delta\hat{\rho}$ in (2.9). Finally, for future use, we define the non-dimensional vaporization rate $\hat{r}$, heat of vaporization $\hat{L}$ and the viscosity μ_0 according to

$$\hat{r} = \tilde{H}\tilde{r}/\tilde{w}_0\tilde{\rho}_{\sigma,0}, \quad \hat{L} = \tilde{L}/\tilde{w}_0^2, \quad \mu_0 = \tilde{\mu}/\tilde{\rho}_0\tilde{w}_0\tilde{H}, \tag{2.11}$$

where the last of these is seen to be the inverse Reynolds number of the steady flow.

We now decompose the dependent variables into a sum of steady and time-dependent (fluctuating) components, anticipating that the steady component can be expanded in powers of δ about the particle-less reference state (2.7) and that the non-steady component can be sought as an expansion in powers of a small parameter $\epsilon = \epsilon(\delta, M)$ that measures the amplitude of the acoustic perturbations and depends on δ and M in a manner to be determined. Thus, according to the scalings described above, we seek a solution in the form

$$p = \gamma^{-1} + M^2 p_s(z) + \not{p}(x, y, z, t) \sim \gamma^{-1} + M^2(\delta p_{s,1} + \ldots) + \epsilon(\not{p}_1 + \epsilon\not{p}_2 + \epsilon^2\not{p}_3 + \ldots), \tag{2.12}$$

$$\rho = \rho_s(z) + \zeta(x, y, z, t) \sim 1 + \delta\rho_{s,1} + \ldots + \epsilon(\zeta_1 + \epsilon\zeta_2 + \epsilon^2\zeta_3 + \ldots), \tag{2.13}$$

$$\rho_\pi = \delta\hat{\rho}_s(z) + \delta\hat{\zeta}(x, y, z, t) \sim \delta\hat{\rho}_{s,1} + \ldots + \delta\epsilon(\hat{\zeta}_1 + \epsilon\hat{\zeta}_2 + \epsilon^2\hat{\zeta}_3 + \ldots), \tag{2.14}$$

$$T = T_s(z) + \theta(x, y, z, t) \sim 1 + \delta T_{s,1} + \ldots + \epsilon(\theta_1 + \epsilon\theta_2 + \epsilon^2\theta_3 + \ldots), \tag{2.15}$$

$$\boldsymbol{u} = M\boldsymbol{u}_s(z) + \boldsymbol{v}(x, y, z, t) \sim M[(0, 0, 1) + (0, 0, \delta w_{s,1}) + \ldots] + \epsilon(\boldsymbol{v}_1 + \epsilon\boldsymbol{v}_2 + \epsilon^2\boldsymbol{v}_3 + \ldots). \tag{2.16}$$

As indicated above, in order to proceed with a formal perturbation analysis of the problem (2.1)–(2.6), it is necessary to relate the orders of magnitude of the three small parameters δ, M and ϵ to one another (§3). It is possible, however, to first calculate the

leading-order coefficients in the steady parts of the expansions and thus determine the leading-order effect of particle loading on the basic solution (i.e. the steady-flow solution in the absence of acoustic perturbations). These coefficients in turn will be needed at higher orders in the analysis of the non-steady problem.

2.3. *The basic solution*

In the absence of acoustic fluctuations, the steady flow solution in the presence of particles is determined by substitution of the steady parts of the expansions (2.12)–(2.16) into the non-dimensional version of the governing equations (2.1)–(2.6) and equating coefficients of like powers of δ. The leading-order solution, which neglects the presence of particles, has already been anticipated by the zeroth-order term in each of the above expansions. The first-order correction is thus determined by $p_{s,1}$, $\rho_{s,1}$, $\hat{\rho}_{s,1}$, $T_{s,1}$ and $w_{s,1}$, which satisfy

$$\frac{\partial \hat{\rho}_{s,1}}{\partial z} = \begin{cases} \hat{r}_0 \equiv \hat{r}(p_s = \gamma^{-1}, T_s = 1) < 0, & \hat{\rho}_{s,1} > 1 \\ 0, & \hat{\rho}_{s,1} = 1, \end{cases} \tag{2.17}$$

$$\frac{\partial}{\partial z}(\rho_{s,1} + w_{s,1}) = \frac{\partial}{\partial z}(\rho_{s,1} + 2w_{s,1} + p_{s,1}) = 0, \tag{2.18a, b}$$

$$\frac{\partial}{\partial z}(p_{s,1} + \gamma w_{s,1} + \hat{\rho}_{s,1}) = \begin{cases} (\gamma - 1)\hat{L}\hat{r}_0, & \hat{\rho}_{s,1} > 1 \\ 0, & \hat{\rho}_{s,1} = 1 \end{cases}, \quad 0 = \rho_{s,1} + T_{s,1} - \hat{\rho}_{s,1}, \tag{2.19a, b}$$

where the fact that $M \ll 1$ has been used to drop the $M^2 p_{s,1}$ term that arises in the $O(\delta)$ equation of state (2.19*b*). The boundary conditions are $p_{s,1} = 0$ at $z = 1$ and $w_{s,1} = T_{s,1} = 0$, $\hat{\rho}_{s,1} = 1 + \lambda$ at $z = 0$, where $\lambda = \tilde{\rho}_{\lambda,0}/\tilde{\rho}_{\sigma,0}$ is the ratio of the liquid to the solid component of the particle density at the point of injection.

We observe from (2.17) that there are two cases to consider, according to whether or not vaporization of the liquid component of the particles goes to completion at a point z_c within the resonance tube ($0 \leqslant z \leqslant 1$). In the first case, the solution for $z \gtrless z_c = z_c^{(0)} + o(1)$, $0 < z_c^{(0)} = -\lambda/\hat{r}_0 < 1$, is

$$\hat{\rho}_{s,1}(z) = \begin{cases} \hat{r}_0 z + 1 + \lambda, \\ 1, \end{cases} \quad w_{s,1} = \left[\hat{L} - \frac{1}{\gamma - 1}\right] \begin{cases} \hat{r}_0 z, \\ -\lambda, \end{cases} \quad T_{s,1} = \left[\hat{L} - \frac{2-\gamma}{\gamma - 1}\right] \begin{cases} \hat{r}_0 z, \\ -\lambda, \end{cases} \tag{2.20a–c}$$

$$p_{s,1} = \left[\hat{L} - \frac{1}{\gamma - 1}\right] \begin{cases} \hat{r}_0(z_c - z), \\ 0, \end{cases} \quad \rho_{s,1} = 1 + \lambda + \left[\hat{L} - \frac{1}{\gamma - 1}\right] \begin{cases} -\hat{r}_0 z, \\ \lambda, \end{cases} \tag{2.20d, e}$$

while for $z_c^{(0)} \geqslant 1$, the corresponding solution for incomplete vaporization is given by (2.20*a–c*) evaluated at $z_c = 1$. We note that the sign of the temperature perturbation $T_{s,1}$ due to the presence of particles is positive or negative depending on whether the (positive) heat of vaporization $\hat{L}$ is less than or greater than $(2-\gamma)/(\gamma-1)$, which for a monatomic ideal gas is $\frac{1}{2}$. Velocity and pressure perturbations have a similar dependence on $\hat{L}$ relative to the larger value $1/(\gamma-1)$, which equals $\frac{3}{2}$ for a monatomic ideal gas.

3. Perturbation analysis

In the presence of time-dependent fluctuations, substitution of the expansions (2.12)–(2.16) into the non-dimensional problem requires that we know how to order terms containing various products of δ, M and ϵ with respect to one another.

Independent of this ordering, however, the leading-order problem for the time-dependent perturbations (consisting of terms of $O(\epsilon)$) decouples into the classical linear acoustics problem for the pressure $\not{p}_1$ and velocity $\boldsymbol{v}_1$ given by

$$\frac{\partial \boldsymbol{v}_1}{\partial t}+\nabla \not{p}_1 = 0, \quad \frac{\partial \not{p}_1}{\partial t}+\nabla\cdot\boldsymbol{v}_1 = 0, \quad \boldsymbol{v}_1|_{z=0} = \not{p}_1|_{z=-1} = \boldsymbol{n}\cdot\boldsymbol{v}_1|_C = 0. \tag{3.1}$$

Nonlinear terms, as well as those proportional to δ and M (such as the non-steady perturbation in the boundary condition at $z = 0$), appear as inhomogeneous terms at higher orders in the analysis and are important in the consideration of the nonlinear acoustics problem to be discussed shortly. Equations (3.1*a*, *b*) can be combined into a single scalar wave equation for either $\not{p}_1$ or a scalar velocity potential (cf. Temkin 1981) which may then be solved by separation of variables. The general oscillatory solution for a rectangular resonance tube of transverse dimensions a and b ($0 \leqslant x \leqslant a$, $0 \leqslant y \leqslant b$) determines the classical acoustic modes

$$\not{p}_1 = \exp(\mathrm{i}\omega_{j,k,l}\, t)\cos(j\pi x/a)\cos(k\pi y/b)\cos[(2l+1)\pi z/2]+\text{c.c.},$$

$\boldsymbol{v}_1 = -\int(\nabla \not{p}_1)\,\mathrm{d}t$, where $\omega^2_{j,k,l} = \pi^2[j^2/a^2+k^2/b^2+(2l+1)^2/4]$ and j, k and l are integers. However, since the higher-frequency modes are highly damped (cf. Margolis 1992*a* or equation (3.12) below), and the interest in the present problem is for the case of relatively long resonance tubes ($a \ll 1, b \ll 1$), only the purely longitudinal, low-frequency modes are important for the present analysis. Thus, for the purposes of this study, the solution to the leading-order problem (3.1) may, for simplicity, be written as a sum over purely longitudinal modes according to

$$\not{p}_1 = \sum_{l=0}^{\infty} A_l \exp(\mathrm{i}\omega_l\, t)\cos[\tfrac{1}{2}(2l+1)\pi z]+\text{c.c.}, \tag{3.2}$$

$$\boldsymbol{v}_1 = (0,0,w_1), \quad w_1 = \sum_{l=0}^{\infty}(-i)\,A_l \exp(\mathrm{i}\omega_l\, t)\sin[\tfrac{1}{2}(2l+1)\pi z]+\text{c.c.}, \tag{3.3}$$

where c.c. denotes the complex conjugate of the preceding term, l is an integer, and the longitudinal acoustic frequencies ω_l are given by

$$\omega_l = \pi(l+\tfrac{1}{2}). \tag{3.4}$$

Thus, the leading-order time-dependent behaviour is that corresponding to the classical acoustic modes. From the non-dimensional versions of (2.2) and (2.3), the corresponding leading-order expressions for the total density and temperature perturbations are found to be given by

$$\zeta_1 = \not{p}_1, \quad \theta_1 = \gamma \not{p}_1 - \zeta_1 = (\gamma-1)\not{p}_1. \tag{3.5a, b}$$

Finally, from (2.1) and the expression for $\hat{\rho}_{\mathrm{s},1}$, we obtain

$$\hat{\zeta}_1 = \begin{cases} \hat{\rho}_{\mathrm{s},1}(z)\not{p}_1 + \hat{r}_0 \displaystyle\sum_{l=0}^{\infty} A_l(\omega_l)^{-1}\exp(\mathrm{i}\omega_l\, t)\sin[\tfrac{1}{2}(2l+1)\pi z]+\text{c.c.}, & z < z_{\mathrm{c}}^{(0)}, \\ \hat{\rho}_{\mathrm{s},1}(z)\not{p}_1, & z \geqslant z_{\mathrm{c}}^{(0)}, \end{cases} \tag{3.5c}$$

where now

$$z_{\mathrm{c}} \sim z_{\mathrm{c}}^{(0)} + \epsilon z_{\mathrm{c}}^{(1)}(t) + \epsilon^2 z_{\mathrm{c}}^{(2)}(t) + \ldots \tag{3.5d}$$

with $z_{\mathrm{c}}^{(0)} = -\lambda/\hat{r}_0$ as before and, through continuity of $\hat{\zeta}_1$ at $z = z_{\mathrm{c}}$,

$$z_{\mathrm{c}}^{(1)} = (\hat{\zeta}_1/\hat{\rho}'_{\mathrm{s},1})|^{z=z_{\mathrm{c}}^{(0)}+}_{z=z_{\mathrm{c}}^{(0)}-} = \hat{r}_0^{-1}\,\hat{\zeta}_1|^{z=z_{\mathrm{c}}^{(0)}+}_{z=z_{\mathrm{c}}^{(0)}-}, \quad z_{\mathrm{c}}^{(2)} = \hat{r}_0^{-1}\,\hat{\zeta}_2|^{z=z_{\mathrm{c}}^{(0)}+}_{z=z_{\mathrm{c}}^{(0)}-} + \hat{r}_0^{-2}(\partial\hat{\zeta}_1/\partial z)|^{z=z_{\mathrm{c}}^{(0)}+}_{z=z_{\mathrm{c}}^{(0)}-}\cdot\hat{\zeta}_1|^{z=z_{\mathrm{c}}^{(0)}+}_{z=z_{\mathrm{c}}^{(0)}-}. \tag{3.5e}$$

Unfortunately, the results (3.1)–(3.5) obtained thus far do little more than give the form of the leading-order solution, since it still remains to determine the (complex)

amplitude A_l of each individual mode and the stability of the corresponding solution. These are determined at higher orders in the analysis by application of solvability conditions on the inhomogeneous terms that appear at those orders. At this point, however, we note that the modal frequencies ω_l are odd multiples of $\frac{1}{2}\pi$, which differ from those obtained in a corresponding analysis of instabilities in rocket motors. There, the boundary condition at $z = 1$ on pressure is usually replaced by a no-penetration condition on velocity (cf. Culick 1990; Culick & Yang 1992), which for the case of purely longitudinal modes, gives modal frequencies which are even multiples of $\frac{1}{2}\pi$.

It is now necessary to relate the three small scales δ, M and ϵ to one another in order to determine which terms appear at which orders in the analysis. The relative magnitude of the steady flow parameters δ and M specifies the level of particle loading relative to the flow rate, and it is clearly possible to consider different regimes. In this work, we consider the regime $\delta \sim M$, in which effects due to a non-zero basic flow velocity and those due to the presence of particles are felt at the same order in the analysis. In that case, a preliminary analysis indicates that, except in special cases as discussed below, the proper scaling of ϵ is $\epsilon \sim M^{\frac{1}{2}}$. Alternatively, choosing ϵ as the single small 'bookkeeping' parameter on which to base our perturbation analysis, we formally introduce the $O(1)$ scaled parameters $\hat{\delta}$ and $\hat{M}$ by defining

$$\delta = \hat{\delta}\epsilon^2, \quad M = \hat{M}\epsilon^2. \tag{3.6}$$

In general, one may anticipate that the evolution of acoustic perturbations occurs on a timescale that is longer than the non-dimensional acoustic scale $\tilde{H}/\tilde{a}_0$ introduced in (2.8). Indeed, a preliminary analysis leads us to introduce the slow time $\tau = \epsilon^2 t$, so that $A_l = A_l(\tau)$. We may now determine evolution equations for these leading-order amplitudes by considering the $O(\epsilon^n)$ problems, where the case $n = 1$ constitutes the homogeneous leading-order problem (3.1), and the higher-order problems are inhomogeneous versions of (3.1). Specifically, for $n \geqslant 2$, the $O(\epsilon^n)$ problems for $\boldsymbol{v}_n$ and $\not{p}_n$ have the form

$$\frac{\partial \boldsymbol{v}_n}{\partial t} + \nabla \not{p}_n = \boldsymbol{r}_n, \quad \frac{\partial \not{p}_n}{\partial t} + \nabla \cdot \boldsymbol{v}_n = q_n, \quad \boldsymbol{v}_n|_{z=0} = (0, 0, b_n), \quad \not{p}_n|_{z=1} = \boldsymbol{n} \cdot \boldsymbol{v}_n|_C = 0, \tag{3.7}$$

where the inhomogeneous terms q_n, $\boldsymbol{r}_n$ and b_n are functions of lower-order coefficients in the expansions (2.12)–(2.16). Then, in order for solutions to the inhomogeneous problems (3.7) to exist, the inhomogeneous terms must satisfy certain solvability conditions at each order. In particular, it is necessary that these terms be orthogonal to all solutions of the homogeneous adjoint problem. Since the homogeneous problem (3.1) is self-adjoint, it is easily shown (Appendix A) that this requirement translates into a set of solvability conditions. For the purely longitudinal oscillations considered here, these conditions are given by

$$\lim_{T \to \infty} \frac{1}{T} \int_0^T \left[\not{p}^\dagger|_{z=0} b_n^* + \int_0^1 (\not{p}^\dagger q_n^* + \boldsymbol{v}_n^\dagger \cdot \boldsymbol{r}_n^*) \, \mathrm{d}z \right] \mathrm{d}t = 0, \tag{3.8}$$

where $\not{p}^\dagger$ and $\boldsymbol{v}^\dagger$ denote any classical acoustic mode (i.e. any term in the solution (3.2)–(3.3)), and the asterisk denotes the complex conjugate. It is the application of (3.8) that ultimately leads to the desired amplitude equations for the leading-order acoustic modes (3.2)–(3.5). We remark that (3.8) is equivalent to, but easier to apply than, a secularity condition that suppresses unbounded growth. This is particularly true when, as in the present problem (see below), it is necessary to go to third (or

higher) order in the analysis. In that case, it is clearly less difficult to apply an integral condition on the inhomogeneous terms at that order than to actually construct the appropriate third-order solutions and then to eliminate those terms that lead to unbounded growth.

At $O(\epsilon^2)$, the expressions for the inhomogeneous terms are given by

$$\boldsymbol{r}_2 = -\zeta_1 \partial \boldsymbol{v}_1/\partial t - (\boldsymbol{v}_1 \cdot \boldsymbol{\nabla})\, \boldsymbol{v}_1, \quad q_2 = -\boldsymbol{v}_1 \cdot \boldsymbol{\nabla} \not{p}_1 - \gamma \not{p}_1 \boldsymbol{\nabla} \cdot \boldsymbol{v}_1, \quad b_2 = 0. \tag{3.9}$$

Application of the solvability conditions then shows that each is identically satisfied unless, for a given index l, there exist either distinct or identical integers l' and l'' such that $\omega_l = \omega_l' \pm \omega_l''$. However, since the ω_l are odd multiples of $\frac{1}{2}\pi$, such a resonant mode interaction, which would first be established on the scale $\epsilon \sim M$ and evolve on the timescale $\tau_1 = \epsilon t$, cannot occur. Consequently, the appropriate procedure is to continue by first constructing the particular solution to the $O(\epsilon^2)$ problem for use in the $O(\epsilon^3)$ problem.

At this point, we pause to emphasizes a fundamental difference between the present problem and, to the best of our knowledge, all nonlinear analyses of the rocket motor stability problem. In the latter, closed exit conditions are used, resulting in a different set of eigenfunctions and corresponding eigenfrequencies from those given above (cf. Culick 1976*a*, *b*; Paparizos & Culick 1989; Yang & Culick 1990). These eigenfrequencies are such that it is possible, as a general rule, for appropriate sums or differences of some of them to equal one of the eigenfrequencies. Consequently, in the present context, a non-trivial solvability condition is always obtained at this order, resulting in quadratic nonlinearities in the resulting amplitude equations. On the other hand, since this does not occur in the present problem, non-trivial solvability conditions are generally not obtained until third order, resulting in cubic nonlinearities in the amplitude equations.

Thus, proceeding to the $O(\epsilon^3)$ problem, the inhomogeneous terms are given by

$$\boldsymbol{r}_3 = -\hat{\delta}\hat{\rho}_{\mathrm{s},1}\frac{\partial \boldsymbol{v}_1}{\partial t} + \hat{M}\left[-\frac{\partial \boldsymbol{v}_1}{\partial z} + \mu_0 \nabla^2 \boldsymbol{v}_1 + \tfrac{1}{3}\mu_0 \boldsymbol{\nabla}(\boldsymbol{\nabla}\cdot\boldsymbol{v}_1)\right] - \frac{\partial \boldsymbol{v}_1}{\partial \tau}$$
$$- \zeta_1(\boldsymbol{v}_1\cdot\boldsymbol{\nabla})\,\boldsymbol{v}_1 - \zeta_2\frac{\partial \boldsymbol{v}_1}{\partial t} - \zeta_1\frac{\partial \boldsymbol{v}_2}{\partial t} - (\boldsymbol{v}_2\cdot\boldsymbol{\nabla})\,\boldsymbol{v}_1 - (\boldsymbol{v}_1\cdot\boldsymbol{\nabla})\,\boldsymbol{v}_2, \tag{3.10a}$$

$$q_3 = -\hat{\delta}\left[(\gamma^{-1}-1)\,\gamma_\pi \hat{\rho}_{\mathrm{s},1}\,\boldsymbol{\nabla}\cdot\boldsymbol{v}_1 + \gamma^{-1}\left(\frac{\partial \hat{\zeta}_1}{\partial t} + \boldsymbol{v}_1\cdot\boldsymbol{\nabla}\hat{\rho}_{\mathrm{s},1}\right)\right] - \hat{M}\frac{\partial \not{p}_1}{\partial z}$$
$$- \frac{\partial \not{p}_1}{\partial \tau} - (\boldsymbol{v}_2\cdot\boldsymbol{\nabla}\not{p}_1 + \boldsymbol{v}_1\cdot\boldsymbol{\nabla}\not{p}_2) - \gamma(\not{p}_2\boldsymbol{\nabla}\cdot\boldsymbol{v}_1 + \not{p}_1\boldsymbol{\nabla}\cdot\boldsymbol{v}_2), \tag{3.10b}$$

$$b_3 = \hat{M} f_0' \not{p}_1|_{z=0,\, t=t-t_{\mathrm{d}}}, \tag{3.10c}$$

where $\gamma_\pi = \tilde{c}_\pi/\tilde{c}_v$ and $f_0' = (\tilde{\rho}_0 \tilde{a}_0^2/\tilde{w}_0)(\mathrm{d}\tilde{f}/\mathrm{d}\tilde{p}|_{\tilde{p}_0}) \sim O(1)$. We note that viscous heating, which is $O(M\epsilon^2) \sim O(\epsilon^4)$, is negligible through this order in the analysis. Application of the solvability conditions at this order then leads to the requirement that the A_l satisfy an infinitely coupled system of evolution equations. These equations take the form

$$\frac{\mathrm{d}A_l}{\mathrm{d}t} = [(\alpha_l + \mu_0\beta_l)M + \gamma_l\delta]\,A_l + \sum_{l'=0}^{\infty}\zeta_{l'}^{l}|A_{l'}|^2 A_l + \sum_{l'=0}^{\infty}\sum_{\substack{l''=0 \\ l''\neq l,\,l'}}^{l+l'}\eta_{l',l'',1}^{l} A_{l'}^{*} A_{l'} A_{l+l'-l''}$$
$$+ \sum_{l'=0}^{\infty}\sum_{l''=0}^{\infty}\eta_{l',l'',2}^{l} A_{l'}^{*} A_{l''}^{*} A_{l+l'+l''+1} + \sum_{l'=0}^{l-1\geqslant 0}\sum_{l''=0}^{l-l'-1}\eta_{l',l'',3}^{l} A_{l'} A_{l''} A_{l-l'-l''-1}, \tag{3.11}$$

where $l = 0, 1, 2, \ldots, \infty$. Note that in writing (3.11), we have skipped a step by writing the amplitude equations in terms of the original unscaled quantities and setting the bookkeeping parameter ϵ equal to unity. (Alternatively, we can simply redefine non-scaled amplitudes $\epsilon A_l \to A_l$ and use the definitions $\tau = \epsilon^2 t$, $\hat{\delta} = \delta/\epsilon^2$, $\hat{M} = M/\epsilon^2$.)

A study of solutions to (3.11) is obviously quite involved, and our preliminary study (Margolis 1992) merely focused on the growth or decay rates of infinitesimal acoustic modes. For the purely longitudinal modes considered here, these are determined by the linearized version of (3.11), which involve only the linear coefficients α_l, β_l and γ_l as calculated from (3.8) and the linear components of (3.10). Indeed, writing the complex amplitudes A_l in the polar form $R_l \exp(\mathrm{i}\phi_l)$, it is readily seen that the real amplitude R_l of an initially infinitesimal acoustic mode will either grow to a finite amplitude determined by the full equations (3.11), or will tend to decay according to whether the linear growth rate $\Delta_l(\delta, M) = \mathrm{Re}\{(\alpha_l + \mu_0 \beta_l) M + \gamma_l \delta\}$ is positive or negative. Here, the γ_l turn out to be purely imaginary, $\alpha_l = f_0' \exp(-\mathrm{i}\omega_l t_\mathrm{d})$, and $\beta_l = -\frac{2}{3}\omega_l^2$. Consequently, the linear growth rate Δ_l of the lth mode is given by

$$\Delta_l = [f_0' \cos(\omega_l t_\mathrm{d}) - \tfrac{2}{3}\mu_0 \omega_l^2] M, \tag{3.12}$$

and so the linear stability of infinitesimal acoustic modes is, in the regime considered here, determined entirely by viscous effects, and by the coupling of the acoustic perturbations in the resonance tube with the incoming flow from the combustion chamber (additional contributions, derived in Appendix B, arise when acoustic boundary effects are considered explicitly, as discussed in §2.1). Clearly, viscous effects (the last term in (3.12)) serve to dampen acoustic perturbations at a rate that increases quadratically with the acoustic frequency. The first term in (3.12), on the other hand, selectively fosters either growth or decay depending on the magnitude of the coupling strength f_0' and the phase difference $\omega_l t_\mathrm{d}$ that relate the third-order (recall $b_1 = b_2 = 0$ in (3.7)) velocity and pressure perturbations at the entrance to the resonance tube. Thus, an acoustic oscillation will be encouraged if the velocity and pressure perturbations are in phase at $z = 0$, and discouraged if the opposite is true, which, if we associate a positive velocity perturbation with additional energy release in the combustion chamber, is in agreement with Rayleigh's classical criterion (Rayleigh 1878). Here, a positive driving of any given acoustic oscillation therefore depends on the value of the time delay t_d. However, since the coupling effects are bounded with respect to frequency, the negative viscous contribution ultimately dominates for sufficiently large frequencies, and thus, as is generally observed, acoustic oscillations are predicted to be dominated by contributions from the lower part of the discrete frequency spectrum.

The focus in the present work is, in contrast to the results just described, on the nonlinear stability of acoustic oscillations for which a consideration of the full, infinitely coupled system (3.11) is necessary. In the next section, we therefore fill in the additional details required to determine actual expressions for the coefficients of the nonlinear terms in these equations.

4. Nonlinear stability of longitudinal modes

Ultimately, we will truncate the amplitude equations (3.11) by retaining only the first N modes (in order of increasing frequency) according to strategies based on the linear results discussed above (see §5). This motivated the anticipated restriction of the analysis to purely longitudinal modes in the previous section for the common case in which the resonance tube is relatively long and narrow. Here, we specialize the analysis

outlined in the previous section further by replacing the infinite summations by finite sums over the leading-order amplitudes A_l, $l = 0, 1, 2, \ldots, N' \equiv N-1$. As a result, the leading-order perturbations (3.1)–(3.5) simplify to

$$\not{p}_1 = \zeta_1 = (\gamma-1)^{-1}\theta_1 = \sum_{l=0}^{N'} A_l \exp(\mathrm{i}\omega_l t)\cos(\omega_l z) + \text{c.c.}, \tag{4.1}$$

$$w_1 = \sum_{l=0}^{N'} (-\mathrm{i})\, A_l \exp(\mathrm{i}\omega_l t)\sin(\omega_l z) + \text{c.c.}, \tag{4.2}$$

$$\hat{\zeta}_1 = \sum_{l=0}^{N'} A_l \exp(\mathrm{i}\omega_l t)\begin{Bmatrix}\hat{\rho}_{\mathrm{s},1}(z)\cos(\omega_l z) + (\hat{r}_0/\omega_l)\sin(\omega_l z)\\ \hat{\rho}_{\mathrm{s},1}(z)\cos(\omega_l z)\end{Bmatrix} + \text{c.c.}, \quad z \lessgtr z_{\mathrm{c}}^{(0)}, \tag{4.3a}$$

$$z_{\mathrm{c}}^{(1)} = -\hat{r}_0 \sum_{l=0}^{N'} A_l \exp(\mathrm{i}\omega_l t)\,\omega_l^{-1}\sin(\omega_l z_{\mathrm{c}}^{(0)}) + \text{c.c.} \tag{4.3b}$$

The determination of the coefficients in the amplitude equations through application of the solvability conditions (3.8) at $O(\epsilon^3)$ requires explicit expressions for the second-order quantities $\not{p}_2$, $\boldsymbol{v}_2 = (0, 0, w_2)$ and ζ_2, which in turn requires that we solve the second-order inhomogeneous problem (3.7) and (3.9). Since the homogeneous solution to that problem is identical in form to the leading-order solution, it is readily seen that it makes no contribution to the solvability condition. The particular solution $\not{p}_2^p$, w_2^p, on the other hand, contains terms proportional to $\exp[\mathrm{i}(\omega_{l'} \pm \omega_{l''})t]$ and their complex conjugates for $l', l'' = 0, 1, \ldots, N'$, and therefore does give a non-trivial contribution to (3.8). Specifically, using standard summation identities for products of sines and/or cosines, the inhomogeneous terms $\boldsymbol{r}_2 = (0, 0, r_2)$ and q_2 become

$$r_2 = \frac{1}{2}\sum_{l'=0}^{N'}\sum_{l''=0}^{N'} \{A_{l'} A_{l''}(\omega_{l'} - \omega_{l''})\exp[\mathrm{i}(\omega_{l'} + \omega_{l''})t] + \text{c.c.} - A_{l'} A_{l''}^{*}(\omega_{l'} + \omega_{l''})$$
$$\times \exp[\mathrm{i}(\omega_{l'} - \omega_{l''})t] + \text{c.c.}\{\sin[(\omega_{l'} + \omega_{l''})z] - \sin[(\omega_{l'} - \omega_{l''})z]\}, \tag{4.4}$$

$$q_2 = \frac{1}{2}\sum_{l'=0}^{N'}\sum_{l''=0}^{N'} \{\mathrm{i}A_{l'} A_{l''}\exp[\mathrm{i}(\omega_{l'} + \omega_{l''})t] + \text{c.c.} + \mathrm{i}A_{l'} A_{l''}^{*}\exp[\mathrm{i}(\omega_{l'} - \omega_{l''})t] + \text{c.c.}\}$$
$$\times \{(\gamma\omega_{l'} + \omega_{l''})\cos[(\omega_{l'} + \omega_{l''})z] + (\gamma\omega_{l'} - \omega_{l''})\cos[(\omega_{l'} - \omega_{l''})z]\}. \tag{4.5}$$

Consequently, it can be verified that w_2^p and $\not{p}_2^p$ are given by

$$\not{p}_2^p = \sum_{l'=0}^{N'}\sum_{l''=0}^{N'} \{A_{l'} A_{l''}[\exp[\mathrm{i}(\omega_{l'} + \omega_{l''})t]\, \Lambda_1^{+}(z; \omega_{l'}, \omega_{l''}) + \text{c.c.}$$
$$+ A_{l'} A_{l''}^{*}\exp[\mathrm{i}(\omega_{l'} - \omega_{l''})t]\, \Lambda_1^{-}(z; \omega_{l'}, \omega_{l''}) + \text{c.c.}\}, \tag{4.6}$$

$$w_2^p = \sum_{l'=0}^{N'}\sum_{l''=0}^{N'} \{A_{l'} A_{l''}[\exp[\mathrm{i}(\omega_{l'} + \omega_{l''})t]\, \Lambda_2^{+}(z; \omega_{l'}, \omega_{l''}) + \text{c.c.}$$
$$+ A_{l'} A_{l''}^{*}\exp[\mathrm{i}(\omega_{l'} - \omega_{l''})t]\, \Lambda_2^{-}(z; \omega_{l'}, \omega_{l''}) + \text{c.c.}\}. \tag{4.7}$$

Here, the z-dependent functions $\Lambda_1^{\pm}$ and $\Lambda_2^{\pm}$ are defined by

$$\Lambda_1^{+}(z; \omega_{l'}, \omega_{l''}) = \gamma^{+}(\omega_{l'})\, z\sin[(\omega_{l'} + \omega_{l''})z]$$
$$+ \hat{\gamma}^{+}(\omega_{l'}, \omega_{l''})\cos[(\omega_{l'} + \omega_{l''})z] + \delta^{+}(\omega_{l'}, \omega_{l''})\cos[(\omega_{l'} - \omega_{l''})z], \tag{4.8}$$

$$\Lambda_2^{+}(z; \omega_{l'}, \omega_{l''}) = \alpha^{+}(\omega_{l'})\, z\cos[(\omega_{l'} + \omega_{l''})z]$$
$$+ \hat{\alpha}^{+}(\omega_{l'}, \omega_{l''})\sin[(\omega_{l'} + \omega_{l''})z] + \beta^{+}(\omega_{l'}, \omega_{l''})\sin[(\omega_{l'} - \omega_{l''})z], \tag{4.9}$$

$$\Lambda_1^{-}(z; \omega_{l'}, \omega_{l''}) = \Lambda_1^{+}(z; \omega_{l'}, -\omega_{l''}), \quad \Lambda_2^{-}(z; \omega_{l'}, \omega_{l''}) = \begin{cases}\Lambda_2^{+}(z; \omega_{l'}, -\omega_{l''}), & l' \neq l'',\\ 0, & l' = l'',\end{cases} \tag{4.10}$$

where

$$\gamma^+(\omega_{l'}) = \tfrac{1}{4}(\gamma+1)\,\omega_{l'}, \quad \hat{\gamma}^+(\omega_{l'},\omega_{l''}) = \delta^+(\omega_{l'},\omega_{l''}) = \frac{\omega_{l'}-\omega_{l''}}{4\omega_{l'}} + (\gamma-1)\frac{\omega_{l'}+\omega_{l''}}{8\omega_{l''}}, \tag{4.11}$$

$$\left.\begin{aligned} \alpha^+(\omega_{l'}) &= \mathrm{i}\gamma^+(\omega_{l'}), \quad \hat{\alpha}^+(\omega_{l'},\omega_{l''}) = \mathrm{i}\left[\frac{(\gamma-1)\,\omega_{l'}+2\omega_{l''}}{4(\omega_{l'}+\omega_{l''})} - \hat{\gamma}^+(\omega_{l'},\omega_{l''})\right], \\ \beta^+(\omega_{l'},\omega_{l''}) &= \mathrm{i}\left[\frac{\omega_{l'}-\omega_{l''}}{4\omega_{l'}} - (\gamma-1)\frac{\omega_{l'}-\omega_{l''}}{8\omega_{l''}}\right]. \end{aligned}\right\} \tag{4.12}$$

Finally, the determination of ζ_2 follows from (2.2) at $O(\epsilon^2)$, which in the general multidimensional case is

$$\frac{\partial\zeta_2}{\partial t} + \nabla\cdot\boldsymbol{v}_2 = -\zeta_1\nabla\cdot\boldsymbol{v}_1 - \boldsymbol{v}_1\cdot\nabla\zeta_1. \tag{4.13}$$

We then use (3.7*b*) and the definition (3.9*b*) for q_2 to note that

$$\nabla\cdot\boldsymbol{v}_2 = -\partial\not{p}_2/\partial t - \boldsymbol{v}_1\cdot\nabla\not{p}_1 - \gamma\not{p}_1\nabla\cdot\boldsymbol{v}_1. \tag{4.14}$$

Substituting this expression for $\nabla\cdot\boldsymbol{v}_2$ into (4.13) and using the fact (equation (4.1)) that $\zeta_1 = \not{p}_1$ thus gives

$$\frac{\partial\zeta_2}{\partial t} = \partial\not{p}_2/\partial t + (\gamma-1)\,\not{p}_1\nabla\cdot\boldsymbol{v}_1. \tag{4.15}$$

Since $\nabla\cdot\boldsymbol{v}_1 = -\partial\not{p}_1/\partial t$ according to (3.1*b*), equation (4.15) may be integrated to yield the long-time result

$$\zeta_2 = \not{p}_2 - \tfrac{1}{2}(\gamma-1)\,\not{p}_1^2, \tag{4.16a}$$

which gives ζ_2 in terms of the first- and second-order pressure perturbations (3.2) and (4.6). In a similar fashion, the second-order particle-density perturbation is determined from (2.1) as

$$\hat{\zeta}_2 = -\hat{\rho}_{\mathrm{s},1}\int(\nabla\cdot\boldsymbol{v}_2)\,\mathrm{d}t - \hat{\rho}'_{\mathrm{s},1}\int w_2\,\mathrm{d}t = \begin{cases} \hat{\rho}_{\mathrm{s},1}(\not{p}_2 - \frac{1}{2}\gamma\not{p}_1^2 - \frac{1}{2}|\boldsymbol{v}_1|^2) - \hat{r}_0\int w_2\,\mathrm{d}t, & z < z_{\mathrm{c}}^{(0)}, \\ \hat{\rho}_{\mathrm{s},1}(\not{p}_2 - \frac{1}{2}\gamma\not{p}_1^2 - \frac{1}{2}|\boldsymbol{v}_1|^2), & z \geqslant z_{\mathrm{c}}^{(0)}, \end{cases} \tag{4.16b}$$

where the second equality follows from (4.14).

Using the first- and second-order solutions obtained above, we may now evaluate the third-order terms $\boldsymbol{r}_3 = (0, 0, r_3)$, q_3 and b_3 given by (3.10). First, we observe that it is only necessary to retain those terms that are proportional to $\exp(\mathrm{i}\omega_l t)$ for $l = 0, 1, \ldots, N'$, since it is only those terms that can give a non-zero contribution to the solvability conditions (3.8). The treatment of the linear terms in (3.10) is straightforward, but the cubic terms require a certain amount of book-keeping. In particular, the evaluation of the latter results in the appearance of triple sums

$$\sum_{l'=0}^{N'}\sum_{l''=0}^{N'}\sum_{l'''=0}^{N'}$$

which are conveniently classified according to the time behaviour of the summands. Specifically, those triple sums whose summands are proportional to one of the seven forms

$$\exp[\mathrm{i}(\omega_{l'}+\omega_{l''}+\omega_{l'''})\,t], \quad \exp[\mathrm{i}(-\omega_{l'}+\omega_{l''}+\omega_{l'''})\,t], \quad \exp[\mathrm{i}(\omega_{l'}-\omega_{l''}+\omega_{l'''})\,t],$$
$$\exp[\mathrm{i}(\omega_{l'}+\omega_{l''}-\omega_{l'''})\,t], \quad \exp[\mathrm{i}(-\omega_{l'}-\omega_{l''}+\omega_{l'''})\,t],$$
$$\exp[\mathrm{i}(\omega_{l'}-\omega_{l''}-\omega_{l'''})\,t], \quad \exp[\mathrm{i}(-\omega_{l'}+\omega_{l''}-\omega_{l'''})\,t]$$

have the potential to give a non-trivial contribution to one of the N solvability conditions (3.8) corresponding to the N adjoint solutions proportional to $\exp(\mathrm{i}\omega_l t)$.

Thus, for a given l, the requirement that the summand be proportional to $\exp(\mathrm{i}\omega_l t)$ results in a double-sum subset of each triple sum that contributes to the corresponding $(l+1)$th solvability condition.

To illustrate these remarks, consider the first of the above seven cases, for which the requirement that $\omega_{l'}+\omega_{l''}+\omega_{l'''}=\omega_l$ implies the restriction $l'+l''+l'''+\frac{3}{2}=l+\frac{1}{2}$, or $l'''=l-(1+l'+l'')$, subject to the original range $0\leqslant l'''\leqslant N'$ for l'''. This in turn restricts l' and l'' to the triangular region $0\leqslant l'\leqslant l-1$, $0\leqslant l''\leqslant l-1-l'$ in the discrete (l',l'')-plane. Clearly, the original triple sum contributes a non-empty double-sum subset $\sum_{l'=0}^{l-1}\sum_{l''=0}^{l-1-l'}$ to all but the first of the N solvability conditions (there is no contribution from this particular case to the first solvability condition corresponding to $l=0$ owing to the fact that it would require l''' to be negative, which is outside its range). The remaining six cases are handled in a similar fashion.

These preliminary considerations thus provide a simple methodology for separating out the non-trivial parts of the inhomogeneous terms. Consequently, writing $r_3=r_3^{\mathrm{l}}+r_3^{\mathrm{nl}}$ and $q_3=q_3^{\mathrm{l}}+q_3^{\mathrm{nl}}$ as sums of linear and nonlinear parts, expressions for b_3 (which is linear), r_3^{l} and q_3^{l} are given in a straightforward fashion from (3.10) by

$$b_3=Mf_0'\sum_{l=0}^{N'}\exp(\mathrm{i}\omega_l t)\,A_l\exp(-\mathrm{i}\omega_l t_{\mathrm{d}})+\mathrm{c.c.} \tag{4.17}$$

$$r_3^{\mathrm{l}}=\sum_{l=0}^{N'}\exp(\mathrm{i}\omega_l t)\left\{\mathrm{i}\frac{\partial A_l}{\partial\tau}\sin(\omega_l z)+\hat{M}A_l\,\mathrm{i}\omega_l[\cos(\omega_l z)+\tfrac{4}{3}\mu_0\omega_l\sin(\omega_l z)]-\hat{\delta}A_l\rho_{\mathrm{s},1}(z)\,\omega_l\sin(\omega_l z)\right\}+\mathrm{c.c.}, \tag{4.18}$$

$$q_3^{\mathrm{l}}=\sum_{l=0}^{N'}\exp(\mathrm{i}\omega_l t)\left\{-\frac{\partial A_l}{\partial\tau}\cos(\omega_l z)+\hat{M}A_l\,\omega_l\sin(\omega_l z)-\hat{\delta}A_l\frac{\mathrm{i}\omega_l}{\gamma}\hat{\rho}_{\mathrm{s},1}(z)[(\gamma-1)\gamma_\pi+1]\cos(\omega_l z)\right\}+\mathrm{c.c.}, \tag{4.19}$$

while expressions for r_3^{nl} and q_3^{nl} are given by

$$\begin{aligned}\begin{Bmatrix}r_3^{\mathrm{nl}}\\ q_3^{\mathrm{nl}}\end{Bmatrix}=\sum_{l=0}^{N'}\exp(\mathrm{i}\omega_l t)\Bigg[&\sum_{l'=0}^{l-1\geqslant 0}\sum_{l''=0}^{l-1-l'}\begin{Bmatrix}a_0(z;\omega_{l'},\omega_{l''},\omega_{l'''})\\ \hat{a}_0(z;\omega_{l'},\omega_{l''},\omega_{l'''})\end{Bmatrix}A_{l'}A_{l''}A_{l'''}|_{l'''=l-1-l'-l''}\\
&+\left(\sum_{l'=0}^{l}\sum_{l''=l-l'}^{N'}+\sum_{l'=l+1\leqslant N'}^{N'}\sum_{l''=0}^{N'+l-l'}\right)\begin{Bmatrix}a_1(z;\omega_{l'},\omega_{l''},\omega_{l'''})\\ \hat{a}_1(z;\omega_{l'},\omega_{l''},\omega_{l'''})\end{Bmatrix}A_{l'}A_{l''}A_{l'''}^*|_{l'''=l'+l''-l}\\
&+\left(\sum_{l'=0}^{l}\sum_{l'''=l-l'}^{N'}+\sum_{l'=l+1\leqslant N'}^{N'}\sum_{l''=0}^{N'+l-l'}\right)\begin{Bmatrix}b_1(z;\omega_{l'},\omega_{l''},\omega_{l'''})\\ \hat{b}_1(z;\omega_{l'},\omega_{l''},\omega_{l'''})\end{Bmatrix}A_{l'}^*A_{l''}A_{l'''}|_{l'=l''+l'''-l}\\
&+\left(\sum_{l'=0}^{l}\sum_{l'''=l-l'}^{N'}+\sum_{l'=l+1\leqslant N'}^{N'}\sum_{l''=0}^{N'+l-l'}\right)\begin{Bmatrix}c_1(z;\omega_{l'},\omega_{l''},\omega_{l'''})\\ \hat{c}_1(z;\omega_{l'},\omega_{l''},\omega_{l'''})\end{Bmatrix}A_{l'}A_{l''}^*A_{l'''}|_{l''=l'+l'''-l}\\
&+\sum_{l'=0}^{N'-l-1\geqslant 0}\sum_{l''=0}^{N'-l-1-l'}\begin{Bmatrix}a_2(z;\omega_{l'},\omega_{l''},\omega_{l'''})\\ \hat{a}_2(z;\omega_{l'},\omega_{l''},\omega_{l'''})\end{Bmatrix}A_{l'}^*A_{l''}^*A_{l'''}|_{l'''=l+1+l'+l''}\\
&+\sum_{l'=0}^{N'-l-1\geqslant 0}\sum_{l'''=0}^{N'-l-1-l''}\begin{Bmatrix}b_2(z;\omega_{l'},\omega_{l''},\omega_{l'''})\\ \hat{b}_2(z;\omega_{l'},\omega_{l''},\omega_{l'''})\end{Bmatrix}A_{l'}A_{l''}^*A_{l'''}^*|_{l''=l+1+l''+l'''}\\
&+\sum_{l'=0}^{N'-l-1\geqslant 0}\sum_{l'''=0}^{N'-l-1-l'}\begin{Bmatrix}c_2(z;\omega_{l'},\omega_{l''},\omega_{l'''})\\ \hat{c}_2(z;\omega_{l'},\omega_{l''},\omega_{l'''})\end{Bmatrix}A_{l'}^*A_{l''}A_{l'''}^*|_{l''=l+1+l'+l'''}\Bigg]+\mathrm{n.c.t.},\end{aligned} \tag{4.20}$$

where n.c.t. (non-contributing terms) stands for all remaining terms that do not contribute to any of the first N solvability conditions. Expressions for the z-dependent

coefficients appearing in (4.20) are given in terms of the functions $\Lambda_{1,2}^{\pm}$ (equations (4.8)–(4.10)) and their derivatives $\Lambda_{1,2}^{\pm\prime} = \mathrm{d}\Lambda_{1,2}^{\pm}/\mathrm{d}z$ according to

$$\left.\begin{matrix} a_0(z;\omega_{l'},\omega_{l''},\omega_{l'''}) \\ a_1(z;\omega_{l'},\omega_{l''},\omega_{l'''}) \end{matrix}\right\} = \omega_{l'''}\cos(\omega_{l'}z)\left[\tfrac{1}{2}(\gamma-1)\cos(\omega_{l''}z)\sin(\omega_{l'''}z) \pm \sin(\omega_{l''}z)\cos(\omega_{l'''}z)\right]$$
$$-\left[\omega_{l'''}\Lambda_1^{+}(z;\omega_{l'},\omega_{l''}) \mp \mathrm{i}\Lambda_2^{+\prime}(z;\omega_{l'},\omega_{l''})\right]\sin(\omega_{l'''}z)$$
$$-\mathrm{i}(\omega_{l'}+\omega_{l''}\mp\omega_{l'''})\,\Lambda_2^{+}(z;\omega_{l'},\omega_{l''})\cos(\omega_{l'''}z), \tag{4.21}$$

$$\left.\begin{matrix} b_2(z;\omega_{l'},\omega_{l''},\omega_{l'''}) \\ c_1(z;\omega_{l'},\omega_{l''},\omega_{l'''}) \end{matrix}\right\} = \omega_{l'''}\cos(\omega_{l'}z)\left[\tfrac{1}{2}(\gamma-1)\cos(\omega_{l''}z)\sin(\omega_{l'''}z) \pm \sin(\omega_{l''}z)\cos(\omega_{l'''}z)\right]$$
$$-\left[\omega_{l'''}\Lambda_1^{-}(z;\omega_{l'},\omega_{l''}) \pm \mathrm{i}\Lambda_2^{-\prime}(z;\omega_{l'},\omega_{l''})\right]\sin(\omega_{l'''}z)$$
$$-\mathrm{i}(\omega_{l'}-\omega_{l''}\pm\omega_{l'''})\,\Lambda_2^{-}(z;\omega_{l'},\omega_{l''})\cos(\omega_{l'''}z), \tag{4.22}$$

$$a_2(z;\omega_{l'},\omega_{l''},\omega_{l'''}) = a_1^{*} = a_1, \quad b_1(z;\omega_{l'},\omega_{l''},\omega_{l'''}) = b_2^{*} = b_2, \quad c_2(z;\omega_{l'},\omega_{l''},\omega_{l'''}) = c_1^{*} = c_1, \tag{4.23}$$

$$\left.\begin{matrix} \hat{a}_0(z;\omega_{l'},\omega_{l''},\omega_{l'''}) \\ \hat{a}_1(z;\omega_{l'},\omega_{l''},\omega_{l'''}) \end{matrix}\right\} = \left[\omega_{l'''}\Lambda_2^{+}(z;\omega_{l'},\omega_{l''}) \pm \mathrm{i}\Lambda_1^{+\prime}(z;\omega_{l'},\omega_{l''})\right]\sin(\omega_{l'''}z)$$
$$-\gamma\left[\Lambda_2^{+\prime}(z;\omega_{l'},\omega_{l''}) \mp \mathrm{i}\omega_{l'''}\Lambda_1^{+}(z;\omega_{l'},\omega_{l''})\right]\cos(\omega_{l'''}z), \tag{4.24}$$

$$\left.\begin{matrix} \hat{b}_2(z;\omega_{l'},\omega_{l''},\omega_{l'''}) \\ \hat{c}_1(z;\omega_{l'},\omega_{l''},\omega_{l'''}) \end{matrix}\right\} = \left[\omega_{l'''}\Lambda_2^{-}(z;\omega_{l'},\omega_{l''}) \mp \mathrm{i}\Lambda_1^{-\prime}(z;\omega_{l'},\omega_{l''})\right]\sin(\omega_{l'''}z)$$
$$-\gamma\left[\Lambda_2^{-\prime}(z;\omega_{l'},\omega_{l''}) \pm \mathrm{i}\omega_{l'''}\Lambda_1^{-}(z;\omega_{l'},\omega_{l''})\right]\cos(\omega_{l'''}z), \tag{4.25}$$

$$\hat{a}_2(z;\omega_{l'},\omega_{l''},\omega_{l'''}) = \hat{a}_1^{*}, \quad \hat{b}_1(z;\omega_{l'},\omega_{l''},\omega_{l'''}) = \hat{b}_2^{*}, \quad \hat{c}_2(z;\omega_{l'},\omega_{l''},\omega_{l'''}) = \hat{c}_1^{*}. \tag{4.26}$$

We observe that since $\Lambda_1^{\pm}$ are strictly real and $\Lambda_2^{\pm}$ are purely imaginary (see equations (4.8)–(4.12)), the coefficients $a_{0,1,2}$, $b_{1,2}$ and $c_{1,2}$ are in fact real, while the coefficients $\hat{a}_{0,1,2}$, $\hat{b}_{1,2}$ and $\hat{c}_{1,2}$ are purely imaginary.

The desired evolution equations for the N unknown amplitudes A_l are now obtained by direct substitution of (4.17)–(4.20) into the solvability conditions (3.8). Transforming back to unscaled variables and parameters (which, as indicated below (3.11), is equivalent to setting the scaling parameter ϵ equal to unity), the result for $l = 0, 1, 2, \ldots, N' = N-1$ is

$$\frac{\mathrm{d}A_l}{\mathrm{d}t} = \left[(\alpha_l+\mu_0\beta_l)M+\gamma_l\delta\right]A_l + \sum_{l'=0}^{l-1\geqslant 0}\sum_{l''=0}^{l-1-l'}\zeta_0(\omega_l,\omega_{l'},\omega_{l''},\omega_{l'''})\,A_{l'}A_{l''}A_{l'''}|_{l'''=l-1-l'-l''}$$
$$+\left(\sum_{l'=0}^{l}\sum_{l''=l-l'}^{N'} + \sum_{l'=l+1\leqslant N'}^{N'}\sum_{l''=0}^{N'+l-l'}\right)\zeta_1(\omega_l,\omega_{l'},\omega_{l''},\omega_{l'''})\,A_{l'}A_{l''}A_{l'''}^{*}|_{l'''=l'+l''-l}$$
$$+\left(\sum_{l''=0}^{l}\sum_{l'''=l-l''}^{N'} + \sum_{l''=l+1\leqslant N'}^{N'}\sum_{l'''=0}^{N'+l-l''}\right)\eta_1(\omega_l,\omega_{l'},\omega_{l''},\omega_{l'''})\,A_{l'}^{*}A_{l''}A_{l'''}|_{l'=l''+l'''-l}$$
$$+\left(\sum_{l'=0}^{l}\sum_{l'''=l-l'}^{N'} + \sum_{l'=l+1\leqslant N'}^{N'}\sum_{l'''=0}^{N'+l-l'}\right)\xi_1(\omega_l,\omega_{l'},\omega_{l''},\omega_{l'''})\,A_{l'}A_{l''}^{*}A_{l'''}|_{l''=l'+l'''-l}$$
$$+\sum_{l'=0}^{N'-l-1\geqslant 0}\sum_{l''=0}^{N'-l-1-l'}\zeta_2(\omega_l,\omega_{l'},\omega_{l''},\omega_{l'''})\,A_{l'}^{*}A_{l''}^{*}A_{l'''}|_{l'''=l+1+l'+l''}$$
$$+\sum_{l''=0}^{N'-l-1\geqslant 0}\sum_{l'''=0}^{N'-l-1-l''}\eta_2(\omega_l,\omega_{l'},\omega_{l''},\omega_{l'''})\,A_{l'}A_{l''}^{*}A_{l'''}^{*}|_{l'=l+1+l''+l'''}$$
$$+\sum_{l'=0}^{N'-l-1\geqslant 0}\sum_{l'''=0}^{N'-l-1-l'}\xi_2(\omega_l,\omega_{l'},\omega_{l''},\omega_{l'''})\,A_{l'}^{*}A_{l''}A_{l'''}^{*}|_{l''=l+1+l'+l'''}, \tag{4.27}$$

where the linear coefficients are given by

$$\alpha_l = f_0' \exp(-\mathrm{i}\omega_l t_\mathrm{d}), \tag{4.28}$$

$$\beta_l = -\tfrac{4}{3}\omega_l^2 \int_0^1 \sin^2(\omega_l z)\,\mathrm{d}z = -\tfrac{2}{3}\omega_l^2, \tag{4.29}$$

$$\gamma_l = -\mathrm{i}\omega_l \int_0^1 \{\rho_{\mathrm{s},1}(z)\sin^2(\omega_l z) + \gamma^{-1}\hat{\rho}_{\mathrm{s},1}(z)[(\gamma-1)\gamma_\pi + 1]\cos^2(\omega_l z)\}\,\mathrm{d}z, \tag{4.30}$$

and the nonlinear coefficients have the representations

$$\zeta_m(\omega_l, \omega_{l'}, \omega_{l''}, \omega_{l'''}) = \int_0^1 [\mathrm{i}a_m(z; \omega_{l'}, \omega_{l''}, \omega_{l'''})\sin(\omega_l z) + \hat{a}_m(z; \omega_{l'}, \omega_{l''}, \omega_{l'''})\cos(\omega_l z)]\,\mathrm{d}z, \tag{4.31a}$$

$$\eta_m(\omega_l, \omega_{l'}, \omega_{l''}, \omega_{l'''}) = \int_0^1 [\mathrm{i}b_m(z; \omega_{l'}, \omega_{l''}, \omega_{l'''})\sin(\omega_l z) + \hat{b}_m(z; \omega_{l'}, \omega_{l''}, \omega_{l'''})\cos(\omega_l z)]\,\mathrm{d}z, \tag{4.31b}$$

$$\xi_m(\omega_l, \omega_{l'}, \omega_{l''}, \omega_{l'''}) = \int_0^1 [\mathrm{i}c_m(z; \omega_{l'}, \omega_{l''}, \omega_{l'''})\sin(\omega_l z) + \hat{c}_m(z; \omega_{l'}, \omega_{l''}, \omega_{l'''})\cos(\omega_l z)]\,\mathrm{d}z, \tag{4.31c}$$

for $m = 0, 1, 2$. Owing to the fact noted above that the a_m, b_m and c_m are real, while the $\hat{a}_m$, $\hat{b}_m$ and $\hat{c}_m$ are imaginary, all of the nonlinear coefficients are also purely imaginary. We remark that the above integrals are readily tractable, but since the resulting expressions are long and are not particularly revealing, we simply leave them in integral form. We also remark that when the nonlinear terms are grouped according to specific products of the amplitudes, additional compactification can be achieved, as indicated by (3.11). However, the coefficients will then consist of various sums of the coefficients defined in (4.31)–(4.33), as shown below for the cases $N = 2$ and $N = 3$. Finally, we emphasize at this point that the nonlinear coefficients depend only on the single parameter γ, the ratio of specific heats for the gas.

5. Truncation strategies

Although the method used to obtain the above amplitude equations is a strictly formal one, at this point the problem is similar to virtually any Galerkin-type approximation in that one must now decide which modes should be kept and which ones can be neglected so as to give an acceptable finite-mode approximation. Rigorous results are elusive and at best appear to establish estimates of lower bounds on the number of modes required for a qualitatively correct approximation (cf. Manley & Trève 1981; Foias & Trève 1981; Trève 1981; Constantin *et al.* 1985). There have also been some attempts to introduce formal procedures for generating sequences of approximations in the vicinity of a bifurcation point (cf. Ingraham 1990), and error-based modifications to the traditional Galerkin approximation have been proposed as well (cf. Foias *et al.* 1988). However, it appears that physically motivated truncation schemes based on a knowledge of linear growth rates remain a reasonable and practical approach, and it is a variant of such a procedure that is adopted here.

The expression (3.12) for the linear growth rates Δ_l indicates that, for a given set of parameter values, only a finite number of modes have positive growth rates, while the

remainder decay at a rate that, generally speaking, increases quadratically with the mode number l. This result is, of course, only accurate for infinitesimal perturbations, but it is logical to anticipate that it is valid in a qualitative sense for finite-amplitude perturbations as well. That is, even though an arbitrarily large number of decaying modes may be excited owing to nonlinear coupling with the linearly unstable, lower-frequency modes, we conjecture that if some form of nonlinear balance is ultimately achieved between growing and decaying modes, the real mode amplitudes $|A_l|$ also will generally decrease with increasing l because as a rule, the larger the mode number, the greater the decay rate per unit amplitude. In physical terms, since $|A_l|^2$ is a relative measure of the energy contained in the lth mode, a bounded solution implies that the unstable lower-frequency modes are able, through nonlinear coupling, to dissipate energy by transferring some of it to the decaying, higher-frequency modes. By the same mechanism, slowly decaying modes, in addition to dissipating energy, also can transfer energy to more rapidly decaying modes. Although energy transfer from a higher- to a lower-frequency mode can, in principle, occur in specific cases (especially if, owing to the sinusoidal term in the expression for the linear growth rate, the former has a smaller rate of decay than the latter), it must be true that the general direction of energy transfer is towards the more dissipative, higher-frequency modes in order for an energy balance to be achieved. Furthermore, the more effective a given mode is at dissipating energy, the smaller the long-time magnitude of the corresponding amplitude is likely to be. The net result is that since amplitudes are expected to generally decay with mode number, it is reasonable to expect that an appropriately truncated version of (3.11), or (4.27) for finite N', will give an approximate solution to the full infinitely coupled system.

Since the modes whose amplitudes are A_l have already been ordered with respect to increasing l, one could, in principle, simply study the problem repeatedly for larger and larger values of the truncation number N until the presumed convergence of any solution becomes apparent. However, we wish to take advantage of our reduction of the original system of conservation laws to a set of ordinary evolution equations (4.27) to obtain, for any given N, the complete bifurcation behaviour of the problem, in as much analytical detail as possible. Thus, we wish to choose a value of N that is as small as possible, but not so small that solutions are spurious (i.e. not preserved for larger values of N) and therefore of no physical interest. Consequently, at the very least, it is obviously appropriate to retain all linearly unstable or neutrally stable modes (i.e. those with non-negative growth rates). However, we also expect, as will be illustrated below, that it is necessary to include one or more modes with negative growth rates in order to provide the stable energy transfer mechanism discussed above. Therefore, our first approximation is to keep a minimum of N modes, where N corresponds to the smallest integer such that the Nth and all higher modes have negative decay rates. Using this rule, there may be one or more modes among the first $N-2$ that have negative decay rates. However, as supported by the analysis below for the case $N = 2$, the preferred direction of energy transfer appears to be from the lower to higher mode numbers, in agreement with similar conclusions drawn in other contexts (cf. Paparizos & Culick 1989). Consequently, it will always be assumed that the Nth mode is a decaying mode, even if one or more lower-frequency decaying modes are already present. Finally, we regard any solution of the N-mode approximation for which A_N is not small, either in magnitude or relative to A_{N-1}, as an indication that this truncation may not be valid with respect to that solution, and proceed to compare the results with those obtained from the $(N+1)$-mode approximation. In contrast, any solution for which A_N is sufficiently small is regarded as a probable approximate

solution of the full amplitude equations, though a comparison with one or more higher-mode approximations is usually still desirable both for qualitative verification and quantitative refinement.

As a final note, we remark that although the analysis that follows indicates that small values of the truncation number N can indeed succeed in capturing the essential bifurcation character of the acoustic oscillations under certain conditions, this is not necessarily the case. For example, although not immediately evident from the two- and three-mode analyses presented below, which are valid when $\Delta_0 > 0$ and $\Delta_{l>0} < 0$, it generally turns out (Margolis 1993) that if $\Delta_l > 0$, there is a strong resonant-type of coupling between the lth mode and the $(3l+1)$th mode corresponding to the frequencies ω_l and $\omega_{3l+1} = 3\omega_l$, respectively. Thus, if the lth mode has a positive linear growth rate, any truncation scheme will need to include the $(3l+1)$th mode, leading to a rapid growth in the truncation number N. For those problems characterized by steep waves or weak shocks, such as the forced piston problem, it is clear that N may have to be quite large to achieve the modal resolution required to capture the phenomenon (cf. Wang & Kassoy 1990*a–c*).

6. Analysis for the case of two modes ($N' = 1$)

Before proceeding, it is convenient to eliminate the Mach number M from (4.27) by re-introducing scaled variables according to

$$\hat{A} = A/M^{\frac{1}{2}}, \quad \tau = Mt, \tag{6.1}$$

which, since $M \sim O(\epsilon^2)$ according to (3.6), essentially corresponds to the same scalings introduced in §§2 and 3. Thus, grouping the nonlinear terms according to products of amplitudes, the two-mode approximation is obtained from (4.27) for $l = 0$ and $l = 1 = N'$ as

$$\frac{\mathrm{d}\hat{A}_0}{\mathrm{d}\tau} = \lambda_0 \hat{A}_0 + \lambda_{0,0,\bar{0}} \hat{A}_0 |\hat{A}_0|^2 + \lambda_{0,1,\bar{1}} \hat{A}_0 |\hat{A}_1|^2 + \lambda_{\bar{0},\bar{0},1} (\hat{A}_0^*)^2 \hat{A}_1, \tag{6.2}$$

$$\frac{\mathrm{d}\hat{A}_1}{\mathrm{d}\tau} = \lambda_1 \hat{A}_1 + \lambda_{0,0,0} \hat{A}_0^3 + \lambda_{0,\bar{0},1} \hat{A}_1 |\hat{A}_0|^2 + \lambda_{1,1,\bar{1}} \hat{A}_1 |\hat{A}_1|^2, \tag{6.3}$$

where the subscripts on the coefficients refer to the particular complex amplitude or set of amplitudes they multiply. They are defined in terms of the original coefficients (4.28)–(4.31) by

$$\lambda_l = \lambda_l^{\mathrm{r}} + \mathrm{i}\lambda_l^{\mathrm{i}} = \alpha_l + \mu_0 \beta_l + \gamma_l \hat{\delta}, \quad \hat{\delta} \equiv \delta/M \sim O(1), \tag{6.4}$$

$$\lambda_{l,l,\bar{l}} = \mathrm{i}\lambda_{l,l,\bar{l}}^{\mathrm{i}} = (\zeta_1 + \eta_1 + \xi_1)(\omega_l, \omega_l, \omega_l, \omega_l) \tag{6.5}$$

for $l = 0$ and 1, and by

$$\lambda_{0,0,0} = \mathrm{i}\lambda_{0,0,0}^{\mathrm{i}} = \zeta_0(\omega_1, \omega_0, \omega_0, \omega_0), \tag{6.6}$$

$$\lambda_{\bar{0},\bar{0},l+1} = \mathrm{i}\lambda_{\bar{0},\bar{0},l+1}^{\mathrm{i}} = \zeta_2(\omega_l, \omega_0, \omega_0, \omega_{l+1}) + \eta_2(\omega_l, \omega_{l+1}, \omega_0, \omega_0) + \xi_2(\omega_l, \omega_0, \omega_{l+1}, \omega_0), \tag{6.7}$$

$$\lambda_{l,l+l'+1,\overline{l+l'+1}} = \mathrm{i}\lambda_{l,l+l'+1,\overline{l+l'+1}}^{\mathrm{i}} = (\zeta_1 + \xi_1)(\omega_l, \omega_l, \omega_{l+l'+1}, \omega_{l+l'+1}) + (\zeta_1 + \eta_1)(\omega_l, \omega_{l+l'+1}, \omega_l, \omega_{l+l'+1}) + (\eta_1 + \xi_1)(\omega_l, \omega_{l+l'+1}, \omega_{l+l'+1}, \omega_l), \tag{6.8}$$

$$\lambda_{l,\bar{l},l+l'+1} = \mathrm{i}\lambda_{l,\bar{l},l+l'+1}^{\mathrm{i}} = (\zeta_1 + \xi_1)(\omega_{l+l'+1}, \omega_{l+l'+1}, \omega_l, \omega_l) + (\zeta_1 + \eta_1)(\omega_{l+l'+1}, \omega_l, \omega_{l+l'+1}, \omega_l) + (\eta_1 + \xi_1)(\omega_{l+l'+1}, \omega_l, \omega_l, \omega_{l+l'+1}), \tag{6.9}$$

for $l = l' = 0$, where, as indicated below (4.31), we have explicitly noted that the complex coefficients of all nonlinear terms have zero real parts. We also observe that the real parts λ_l^{r} of the linear coefficients are equal to the scaled linear growth rates $M^{-1}\Delta_l$. In accordance with the discussion in §5, we assume, unless otherwise noted, that $\lambda_0^{\mathrm{r}} > 0$ and $\lambda_1^{\mathrm{r}} < 0$, corresponding to a linearly unstable first mode and a linearly stable second mode.

In proceeding with an analysis of (6.2) and (6.3), it is convenient to introduce real amplitudes and phases for the complex amplitudes $\hat{A}_l(\tau) = R_l(\tau)\exp[\mathrm{i}\phi_l(\tau)]$. Substituting this representation into the complex amplitude equations and separating real and imaginary parts then leads to the equivalent system

$$\frac{\mathrm{d}R_0}{\mathrm{d}\tau} = \lambda_0^{\mathrm{r}} R_0 - \lambda^{\mathrm{i}}_{\bar{0},\bar{0},1} R_0^2 R_1 \sin(\phi_1 - 3\phi_0), \tag{6.10}$$

$$\frac{\mathrm{d}R_1}{\mathrm{d}\tau} = \lambda_1^{\mathrm{r}} R_1 + \lambda^{\mathrm{i}}_{0,0,0} R_0^3 \sin(\phi_1 - 3\phi_0), \tag{6.11}$$

$$R_0 \frac{\mathrm{d}\phi_0}{\mathrm{d}\tau} = \lambda_0^{\mathrm{i}} R_0 + \lambda^{\mathrm{i}}_{0,0,\bar{0}} R_0^3 + \lambda^{\mathrm{i}}_{0,1,\bar{1}} R_0 R_1^2 + \lambda^{\mathrm{i}}_{\bar{0},\bar{0},1} R_0^2 R_1 \cos(\phi_1 - 3\phi_0), \tag{6.12}$$

$$R_1 \frac{\mathrm{d}\phi_1}{\mathrm{d}\tau} = \lambda_1^{\mathrm{i}} R_1 + \lambda^{\mathrm{i}}_{0,0,0} R_0^3 \cos(\phi_1 - 3\phi_0) + \lambda^{\mathrm{i}}_{0,\bar{0},1} R_0^2 R_1 + \lambda^{\mathrm{i}}_{1,1,\bar{1}} R_1^3. \tag{6.13}$$

By introducing the phase difference variable $\psi \equiv \phi_1 - 3\phi_0$, we thus obtain the closed subsystem

$$\frac{\mathrm{d}R_0}{\mathrm{d}\tau} = \lambda_0^{\mathrm{r}} R_0 - \lambda^{\mathrm{i}}_{\bar{0},\bar{0},1} R_0^2 R_1 \sin\psi, \tag{6.14}$$

$$\frac{\mathrm{d}R_1}{\mathrm{d}\tau} = \lambda_1^{\mathrm{r}} R_1 + \lambda^{\mathrm{i}}_{0,0,0} R_0^3 \sin\psi, \tag{6.15}$$

$$\frac{\mathrm{d}\psi}{\mathrm{d}\tau} = \lambda_d + \lambda_p R_0^2 + \lambda_q R_1^2 + \lambda^{\mathrm{i}}_{0,0,0} R_0^3 R_1^{-1} \cos\psi - 3\lambda^{\mathrm{i}}_{\bar{0},\bar{0},1} R_0 R_1 \cos\psi, \tag{6.16}$$

where we have defined

$$\lambda_d \equiv \lambda_1^{\mathrm{i}} - 3\lambda_0^{\mathrm{i}}, \quad \lambda_p \equiv \lambda^{\mathrm{i}}_{0,\bar{0},1} - 3\lambda^{\mathrm{i}}_{0,0,\bar{0}}, \quad \lambda_q \equiv \lambda^{\mathrm{i}}_{1,1,\bar{1}} - 3\lambda^{\mathrm{i}}_{0,1,\bar{1}}. \tag{6.17}$$

Although not immediately obvious, it can be shown that the coefficients of the nonlinear terms, which are functions of γ only, are related to one another according to

$$\lambda^{\mathrm{i}}_{\bar{0},\bar{0},1} = \lambda^{\mathrm{i}}_{0,0,0}, \quad \lambda^{\mathrm{i}}_{0,\bar{0},1} = 3\lambda^{\mathrm{i}}_{0,1,\bar{1}}, \quad \lambda^{\mathrm{i}}_{1,1,\bar{1}} = 3\lambda^{\mathrm{i}}_{0,0,\bar{0}}, \quad \lambda_p = -\lambda_q = 3\lambda^{\mathrm{i}}_{0,0,0}. \tag{6.18a–d}$$

Thus, the number of parameter-dependent coefficients in (6.14)–(6.16) actually reduces to the real part of the linear growth rates λ_0^{r} and λ_1^{r}, a phase difference λ_d formed from the imaginary parts of the linear growth rates, and a single nonlinear coefficient $\lambda^{\mathrm{i}}_{0,0,0}(\gamma)$ that is independent of any coupling or particle parameters. Fur future reference, $\lambda^{\mathrm{i}}_{0,0,0}$ and $\lambda^{\mathrm{i}}_{0,0,\bar{0}}$ are plotted in figure 2, where the latter is needed in the calculation of the individual phases ϕ_1 and ϕ_2. The remaining nonlinear coefficients are then completely determined according to (6.18).

Equations (6.14)–(6.16) allow us to verify immediately several of the conjectures discussed in §5 that guide our choice of a first truncated approximation of the

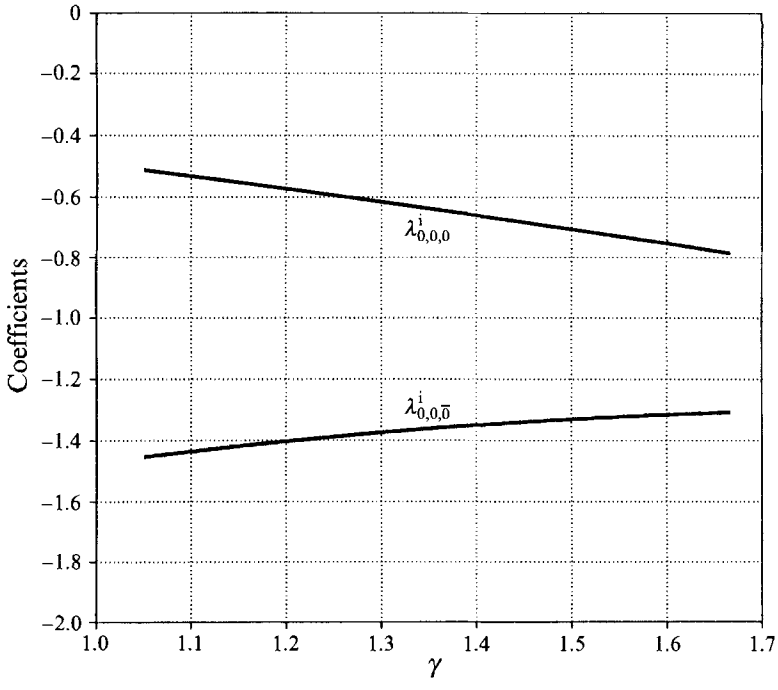

FIGURE 2. The nonlinear coefficients $\lambda^{i}_{0,0,0}$ $(=\lambda^{i}_{\bar{0},\bar{0},1})$ and $\lambda^{i}_{0,0,\bar{0}}$ $(=\frac{1}{3}\lambda^{i}_{1,1,\bar{1}})$ as functions of their only parameter γ.

amplitude equations. First, if we had retained only the first unstable mode, then (6.14) for R_0 would have been simply $\mathrm{d}R_0/\mathrm{d}\tau = \lambda^{r}_{0} R_0$, which leads to unbounded growth for $\lambda^{r}_{0} > 0$. Thus, as conjectured, it is clearly necessary to retain at least one stable mode in order to provide the coupling necessary for a balance between growing and decaying modes. Secondly, if we had assumed that the first mode was stable and the second mode was unstable (i.e. $\lambda^{r}_{0} < 0$, $\lambda^{r}_{1} > 0$), then the above two-mode approximation admits the unbounded solution $R_0 = 0$, $R_1 = \exp(\lambda^{r}_{1} t) \to \infty$. Hence, even though a decaying mode was retained in the truncated equations, the fact that it corresponds to a lower frequency results in an inability of the system to maintain the necessary balance between the growing and decaying modes. On the other hand, when $\lambda^{r}_{0} > 0$ and $\lambda^{r}_{1} < 0$, a long-time solution of the form $R_0 \neq 0$, $R_1 = 0$ does not exist, and indeed we shall see that a nonlinear balance is possible only for non-zero values of both modes. In other words, the transfer of energy from the growing to the decaying modes is more effective when the direction of transfer is up, rather than down, the frequency spectrum, as suggested in §5.

We now look for steady solutions of (6.14)–(6.16). Since the individual phases will then grow linearly in time according to (6.12) and (6.13), such solutions in fact correspond to time-periodic solutions of the complex amplitude equations (6.2) and (6.3). In particular, these solutions will describe limit cycles with perturbed modal frequencies $\varpi_0 \approx \omega_0 + M^2 \mathrm{d}\phi_0/\mathrm{d}t$ and $\varpi_1 \approx \omega_1 + M^2 \mathrm{d}\phi_1/\mathrm{d}t, = 3\varpi_0$, where the last equality follows from $\omega_1 = \frac{3}{2}\pi = 3\omega_0$ and $\mathrm{d}\psi/\mathrm{d}t = \mathrm{d}(\phi_1 - 3\phi_0)/\mathrm{d}t = 0$.

To analyse the steady solution behaviour of (6.14)–(6.16), it is convenient to first define new variables according to

$$z_0 \equiv R_0^2, \quad z_1 \equiv R_1^2, \quad x \equiv R_0 R_1 \cos\psi, \quad y \equiv R_0 R_1 \sin\psi. \qquad (6.19a\text{–}d)$$

Then, multiplying (6.14) by R_0, (6.15) by R_1, and (6.16) by R_1^2, the steady-state version of these equations becomes

$$0 = \lambda_0^{\mathrm{r}} - \lambda^{\mathrm{i}}_{\bar{0},\bar{0},1}\, y, \tag{6.20}$$

$$0 = \lambda_1^{\mathrm{r}} z_1 + \lambda^{\mathrm{i}}_{0,0,0}\, z_0 y, \tag{6.21}$$

$$0 = \lambda_d z_1 + \lambda_q z_1^2 + \lambda_p z_0 z_1 + \lambda^{\mathrm{i}}_{0,0,0}\, z_0 x - 3\lambda^{\mathrm{i}}_{\bar{0},\bar{0},1}\, z_1 x, \tag{6.22}$$

$$x^2 + y^2 = z_0 z_1, \tag{6.23}$$

where the last follows from the definitions of x and y in (6.19). These are four nonlinear algebraic equations in four unknowns, the first of which gives

$$y = \lambda_0^{\mathrm{r}} / \lambda^{\mathrm{i}}_{\bar{0},\bar{0},1}. \tag{6.24}$$

Then, from (6.21), we have the relationship

$$z_1 = \kappa^2 z_0, \quad \kappa^2 \equiv -\frac{\lambda_0^{\mathrm{r}} \lambda^{\mathrm{i}}_{0,0,0}}{\lambda_1^{\mathrm{r}} \lambda^{\mathrm{i}}_{\bar{0},\bar{0},1}} > 0, \tag{6.25}$$

where, since z_1 and z_2 are positive, the inequality is a necessary condition for a non-trivial solution to exist. As noted in (6.18*a*), it is in fact the case that $\lambda^{\mathrm{i}}_{0,0,0} = \lambda^{\mathrm{i}}_{\bar{0},\bar{0},1}$, and so this necessary condition requires that the linear growth rates λ_0^{r} and λ_1^{r} must have opposite signs. We may therefore anticipate from (6.25), as will be demonstrated below, that the limit cycle bifurcates from the trivial solution at $\lambda_0^{\mathrm{r}} = 0$, and that the bifurcation is supercritical. When both modes are linearly unstable, the two-mode analysis is incapable of describing a steady limit cycle, which again supports the conjecture that any truncation which does not include decaying modes is not a valid approximation. Finally, from (6.23) and (6.25), we have

$$x = \pm(\kappa^2 z_0^2 - y^2)^{\frac{1}{2}}, \tag{6.26}$$

with the sign of x still to be determined.

Using these relationships, non-trivial solutions for z_0 are now determined implicitly from (6.22) according to

$$\lambda_d + (\lambda_q \kappa^2 + \lambda_p) z_0 = \operatorname{sgn}(x)\, \lambda^{\mathrm{i}}_{\bar{0},\bar{0},1} (3 + \lambda_1^{\mathrm{r}}/\lambda_0^{\mathrm{r}}) [\kappa^2 z_0^2 - (\lambda_0^{\mathrm{r}}/\lambda^{\mathrm{i}}_{\bar{0},\bar{0},1})^2]^{\frac{1}{2}}. \tag{6.27}$$

Squaring both sides of (6.27), we see that for given parameter values, there can exist zero, one or two real positive solutions determined by a quadratic equation for z_0 given by

$$[(\kappa^2 \lambda_q + \lambda_p)^2 - (\kappa \lambda^{\mathrm{i}}_{\bar{0},\bar{0},1})^2 (3 + \lambda_1^{\mathrm{r}}/\lambda_0^{\mathrm{r}})^2] z_0^2 + 2\lambda_d (\kappa^2 \lambda_q + \lambda_p) z_0 + \lambda_d^2 + (3\lambda_0^{\mathrm{r}} + \lambda_1^{\mathrm{r}})^2 = 0, \tag{6.28}$$

subject to the restriction, imposed by (6.26), that $z_0^2 \geqslant y^2/\kappa^2 = -\lambda_0^{\mathrm{r}} \lambda_1^{\mathrm{r}} / \lambda^{\mathrm{i}}_{0,0,0} \lambda^{\mathrm{i}}_{\bar{0},\bar{0},1}$. The sign of x for any solution is then determined from (6.27), which, from (6.20), the definition (6.19*d*) for y, and (6.25), uniquely determines the phase variable ψ as

$$\psi = \begin{cases} \psi_p, & \operatorname{sgn}(x) > 0 \\ \pi - \psi_p, & \operatorname{sgn}(x) < 0 \end{cases}, \quad \psi_p = \arcsin\left(\frac{\lambda_0^{\mathrm{r}}}{\kappa \lambda^{\mathrm{i}}_{\bar{0},\bar{0},1} z_0}\right). \tag{6.29}$$

According to these results, as one or more parameters are varied so that λ_0^{r} increases past zero, an acoustic oscillation bifurcates supercritically from the basic unperturbed flow. Indeed, in the neighbourhood of the bifurcation point ($0 < \lambda_0^{\mathrm{r}} \ll 1$), the solution behaves as

$$z_0 = \frac{(|\lambda_1^{\mathrm{r}}| + \lambda_d^2/|\lambda_1^{\mathrm{r}}|)^{\frac{1}{2}}}{|\lambda^{\mathrm{i}}_{0,0,0}|} (\lambda_0^{\mathrm{r}})^{\frac{1}{2}} + O(\lambda_0^{\mathrm{r}}), \quad z_1 = \lambda_0^{\mathrm{r}} z_0 / |\lambda_1^{\mathrm{r}}| \sim O(\lambda_0^{\mathrm{r}})^{\frac{3}{2}}, \quad x = \frac{\lambda_d}{|\lambda_1^{\mathrm{r}}|\, \lambda^{\mathrm{i}}_{0,0,0}} \lambda_0^{\mathrm{r}} + O(\lambda_0^{\mathrm{r}})^{\frac{3}{2}}, \tag{6.30}$$

where we have used the fact noted above that $\lambda^{\mathrm{i}}_{0,0,0}/\lambda^{\mathrm{i}}_{\bar{0},\bar{0},1} = 1$. We observe that near the bifurcation point, $z_1/z_0 \sim O(\lambda^{\mathrm{r}}_0) \ll 1$, which is consistent with a two-mode analysis. Indeed, the accuracy of any solution for which this ratio is not small is immediately suspect, since it indicates the need to retain additional decaying modes in the truncation scheme. However, $O(1)$ values of this ratio may still be qualitatively valid. Large values of this ratio, on the other hand, are unacceptable, and may in fact be spurious in the sense that they disappear when additional modes are included. For example, in the limit $|\lambda^{\mathrm{r}}_1| \to 0$ (i.e. in the limit that the decay rate of the stable mode becomes small), (6.25) implies that z_1/z_0 becomes unbounded. In order to describe possible solutions in this parameter regime, a higher-order truncation scheme is clearly required.

The local stability of a steady solution $R^{\mathrm{s}}_0 = (z_0)^{\frac{1}{2}}$, $R^{\mathrm{s}}_1 = (z_1)^{\frac{1}{2}}$, ψ^{s} (or x^{s}) is determined by a linear stability analysis of (6.14)–(6.16). In particular, using the relationships (6.19), (6.24) and (6.25), the linear stability of this solution is determined by the eigenvalues of the stability matrix

$$\begin{bmatrix} -\lambda^{\mathrm{r}}_0 & -\lambda^{\mathrm{r}}_0/\kappa & \\ -3\kappa\lambda^{\mathrm{r}}_1 & \lambda^{\mathrm{r}}_1 & \\ 2\lambda_p R^{\mathrm{s}}_0 - 3\lambda^{\mathrm{i}}_{\bar{0},\bar{0},1}(1+\lambda^{\mathrm{r}}_1/\lambda^{\mathrm{r}}_0) R^{\mathrm{s}}_1 \cos\psi^{\mathrm{s}} & 2\lambda_q R^{\mathrm{s}}_1 - \lambda^{\mathrm{i}}_{\bar{0},\bar{0},1}(3-\lambda^{\mathrm{r}}_1/\lambda^{\mathrm{r}}_0) R^{\mathrm{s}}_0 \cos\psi^{\mathrm{s}} & -\lambda^{\mathrm{i}}_{\bar{0},\bar{0},1} R^{\mathrm{s}^2}_0 R^{\mathrm{s}}_1 \cos\psi^{\mathrm{s}} \\ & & \lambda^{\mathrm{i}}_{0,0,0} R^{\mathrm{s}^3}_0 \cos\psi^{\mathrm{s}} \\ & & 3\lambda^{\mathrm{r}}_0 + \lambda^{\mathrm{r}}_1 \end{bmatrix}, \tag{6.31}$$

where positive (negative) eigenvalues correspond to growth (decay) of infinitesimal perturbations $r_0 = R_0 - R^{\mathrm{s}}_0$, $r_1 = R_1 - R^{\mathrm{s}}_1$ and $\varphi = \psi - \psi^{\mathrm{s}}$. From the behaviour (6.30), it can be shown that in the neighbourhood of the bifurcation point ($0 < \lambda^{\mathrm{r}}_0 \ll 1$), the eigenvalues ($\Lambda_1, \Lambda_2, \Lambda_3$) of the stability matrix behave as

$$\Lambda_{1,2} = -|\lambda^{\mathrm{r}}_1| \pm \mathrm{i}\,(\lambda^2_a/|\lambda^{\mathrm{i}}_{0,0,0}|)^{\frac{1}{2}} + O(\lambda^{\mathrm{r}}_0), \quad \Lambda_3 \sim -4\lambda^{\mathrm{r}}_0. \tag{6.32}$$

Consequently, since the real parts are negative, the limit cycle is stable as it bifurcates from the basic flow solution, which loses stability, at $\lambda^{\mathrm{r}}_0 = f'_0 \cos(\omega_0 t_{\mathrm{d}}) - 2\mu_0\omega^2_0/3 = 0$, or equivalently, as the reduced parameter $\mathscr{F} \equiv f'_0 \cos(\omega_0 t_{\mathrm{d}})/\mu_0$ crosses the critical value $\mathscr{F}_0 = \frac{2}{3}\omega^2_0 = \frac{1}{6}\pi^2 \doteq 1.644934$. We note that in terms of this parameter,

$$\lambda^{\mathrm{r}}_0 = \mu_0(\mathscr{F} - \tfrac{2}{3}\omega^2_0) = \mu_0(\mathscr{F} - \tfrac{1}{6}\pi^2), \tag{6.33a}$$

$$\lambda^{\mathrm{r}}_1 = f'_0 \cos(\omega_1 t_{\mathrm{d}}) - \tfrac{2}{3}\mu_0\omega^2_1 = \mu_0\left[\mathscr{F}\frac{\cos(3\omega_0 t_{\mathrm{d}})}{\cos(\omega_0 t_{\mathrm{d}})} - 6\omega^2_0\right] = \mu_0\{[4\cos^2(\tfrac{1}{2}\pi t_{\mathrm{d}}) - 3]\,\mathscr{F} - \tfrac{3}{2}\pi^2\}. \tag{6.33b}$$

Thus, as required, $\lambda_1 < 0$ is negative at the bifurcation point $\mathscr{F} = \mathscr{F}_0$, but can cross from negative to positive values at the larger value $\mathscr{F}_1 = \frac{3}{2}\pi^2/[4\cos^2(\frac{1}{2}\pi t_{\mathrm{d}}) - 3]$. Since we have already shown the bifurcation to be supercritical (i.e. $\lambda^{\mathrm{r}}_0 > 0$, which requires that $\mathscr{F}$ be positive), we may restrict further consideration to the range $-\frac{1}{2}\pi < \omega_0 t_{\mathrm{d}} < \frac{1}{2}\pi$ (i.e. $-1 < t_{\mathrm{d}} < 1$, which ensures that $\mathscr{F} > 0$). Consequently, for time delays in the range $0 \leqslant |t_{\mathrm{d}}| \leqslant \frac{1}{3}$, $\mathscr{F}_1$ lies in the range $\frac{3}{2}\pi^2 = 9\mathscr{F}_0 \leqslant \mathscr{F}_1 \leqslant \infty$, while larger values of $|t_{\mathrm{d}}| < 1$ imply that λ^{r}_1 remains negative for all $\mathscr{F} > 0$.

Bifurcation diagrams corresponding to solutions of (6.28) as the coupling strength f'_0 increases are shown in figures 3–9. They depend on all of the parameters

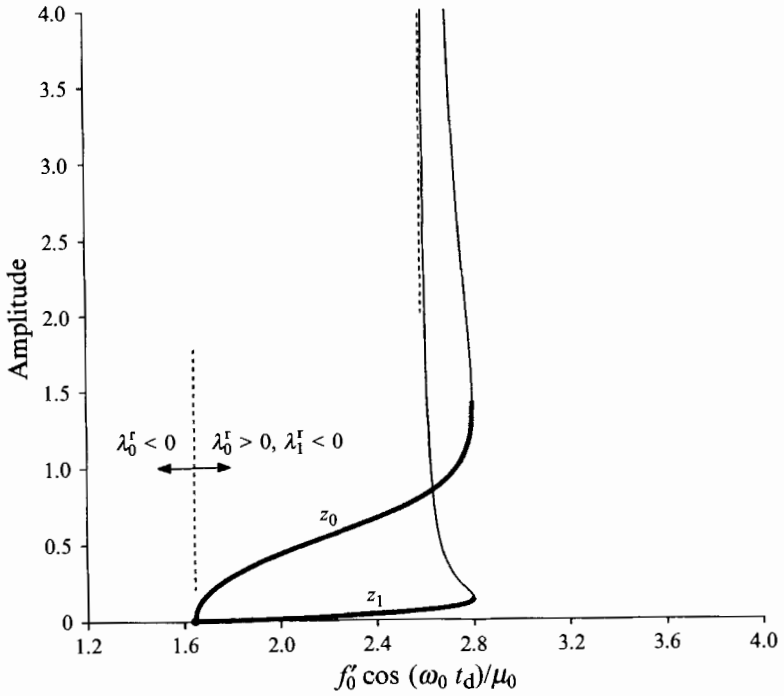

FIGURE 3. Acoustic amplitudes $z_0 = R_0^2$ and $z_1 = R_1^2$ as a function of the parameter group $\mathscr{F} = f_0' \cos(\omega_0 t_d)/\mu_0$ in the two-mode approximation. Heavy (light) curves denote stable (unstable) branches. Parameter values are $\gamma = 1.3$, $\mu_0 = \frac{1}{8}$, $t_d = 0$, and typical values of particle-related parameters (quoted in the text).

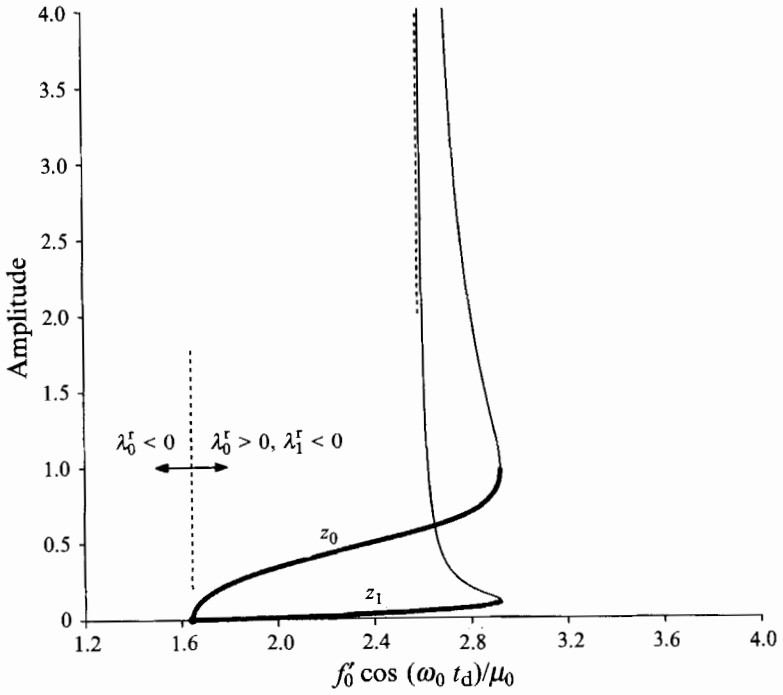

FIGURE 4. Same as figure 3 with $\gamma = \frac{5}{3}$.

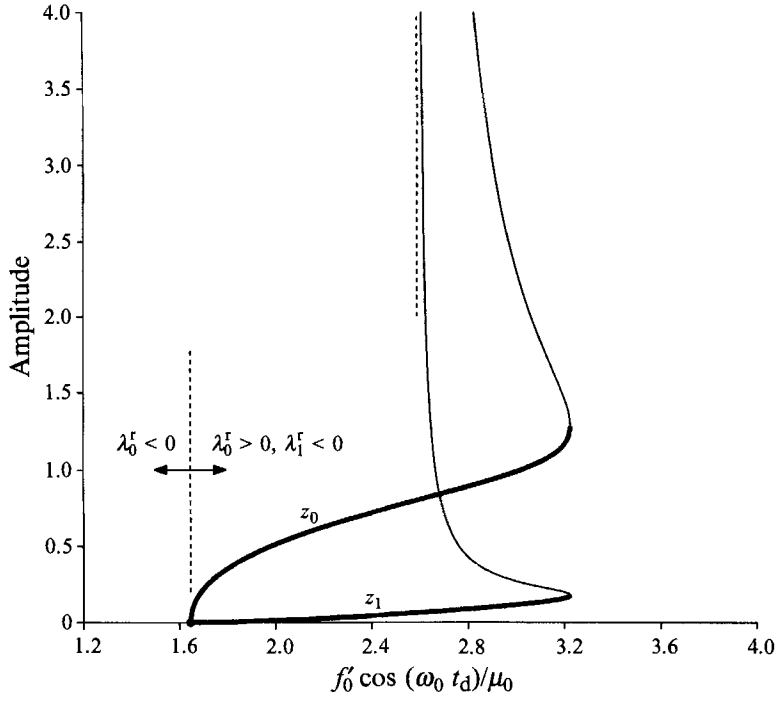

FIGURE 5. Same as figure 3 with $\gamma = 1.1$.

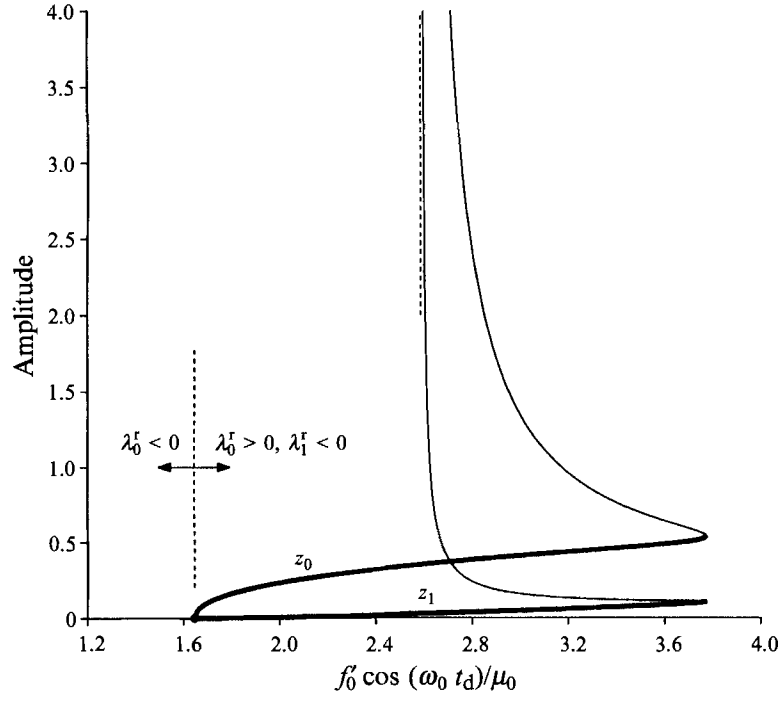

FIGURE 6. Same as figure 3 with $\mu_0 = \frac{1}{16}$.

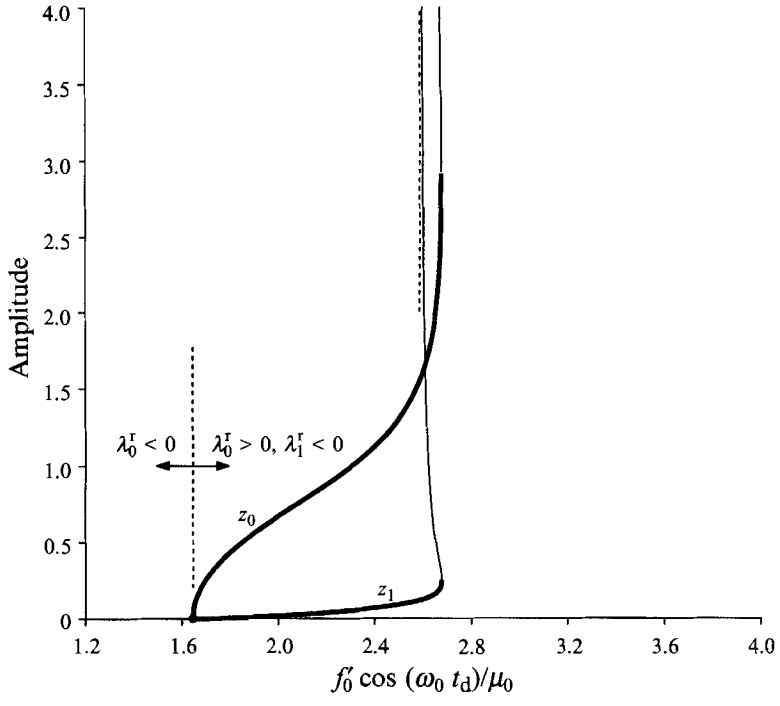

FIGURE 7. Same as figure 3 with $\mu_0 = \frac{3}{16}$.

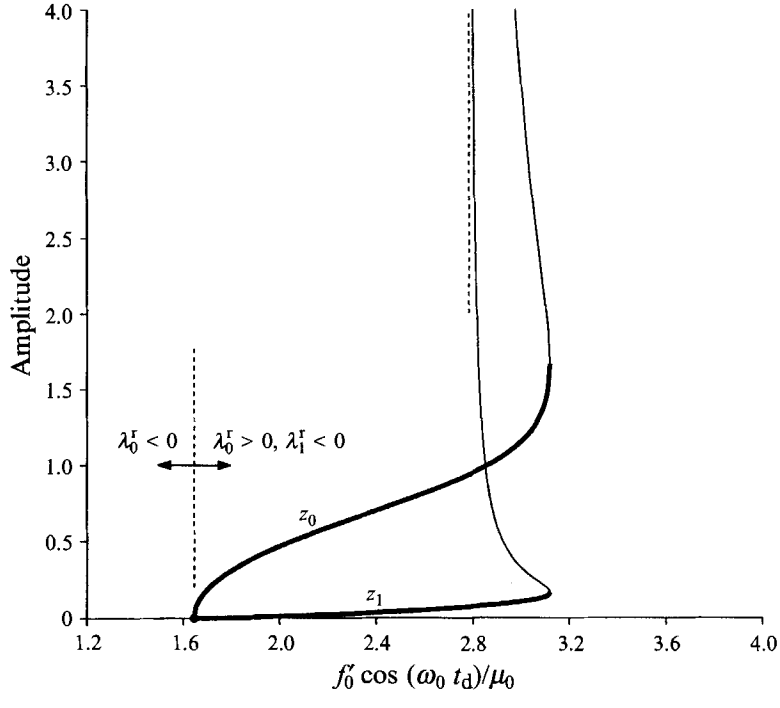

FIGURE 8. Same as figure 3 with $t_d = \frac{1}{3}$ (i.e. $\omega_0 t_d = \frac{1}{6}\pi, \omega_1 t_d = \frac{1}{2}\pi$).

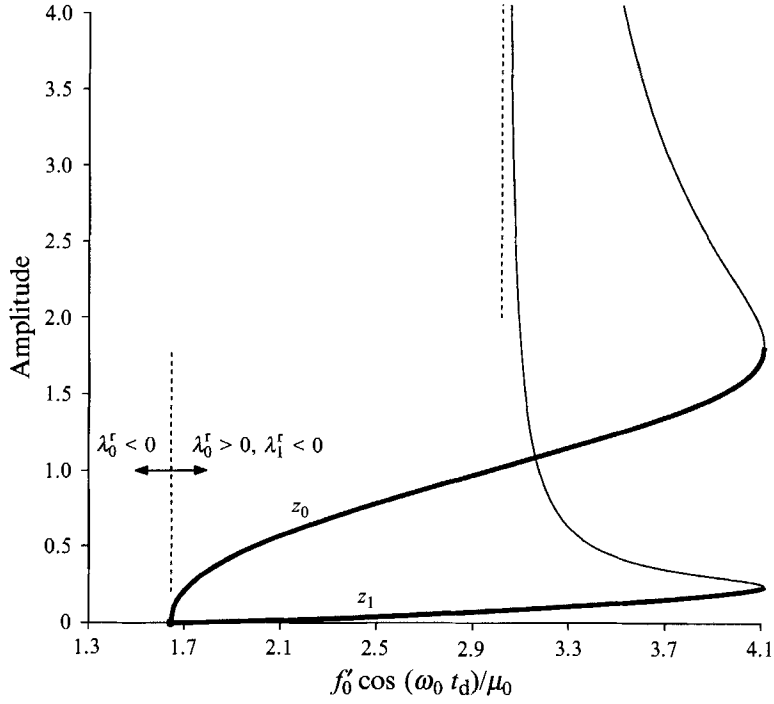

FIGURE 9. Same as figure 3 with $t_d = \frac{1}{2}$ (i.e. $\omega_0 t_d = \frac{1}{4}\pi, \omega_1 t_d = \frac{3}{4}\pi$).

individually, but by plotting the amplitudes $z_0 = R_0^2$, $z_1 = R_1^2$ against the reduced parameter group $\mathscr{F}$, we preserve the bifurcation point at the same value $\mathscr{F} = \mathscr{F}_0 = \frac{1}{6}\pi^2$ as discussed above. In the neighbourhood of the bifurcation point, the limit cycle has the local behaviour described by (6.30). As f_0' increases, the amplitudes grow until eventually a turning point $\mathscr{F} = \mathscr{F}_c$ is reached that corresponds to the vanishing of the discriminant in the solution of the quadratic (6.28). At this point, which also corresponds to a zero eigenvalue of the stability matrix (6.30), the bifurcation branch loses stability, and thus only the lower branch is stable. For f_0' greater than this critical value, no steady solutions are obtained, and indeed a numerical integration of the time-dependent amplitude equations (6.14)–(6.16) shows that solutions grow unbounded in time. In other words, for sufficiently strong coupling, energy cannot be transferred to and/or dissipated by the decaying mode fast enough for acoustic oscillations to remain bounded (in §7, we argue that this qualitative result can be physical, and is not necessarily an artificial consequence of not retaining enough decaying modes). Much larger values of the coupling parameter, however, resulted in a pair of additional branches that are born at a second critical value of the coupling parameter (figure 10). However, they correspond to solutions for which $z_1/z_0 \sim O(1)$ or larger and which disappear in the three-mode approximation (§7). They are therefore unphysical and we conclude that in the parameter regime in which they are found, the two-mode approximation is no longer valid, even though this regime still corresponds to $\lambda_1^r < 0$. The branches shown in figures 3–9 for smaller values of f_0', on the other hand, not only satisfy the expectation that z_1/z_0 be small, but are also preserved in the higher-mode approximation, and we therefore regard these as physical.

Figures 3–9 also allow a comparison of the amplitudes and the critical values of the coupling parameter beyond which the limit cycle does not exist, at least in this approximation. Figures 3–5 compare different values of the ratio of specific heats γ,

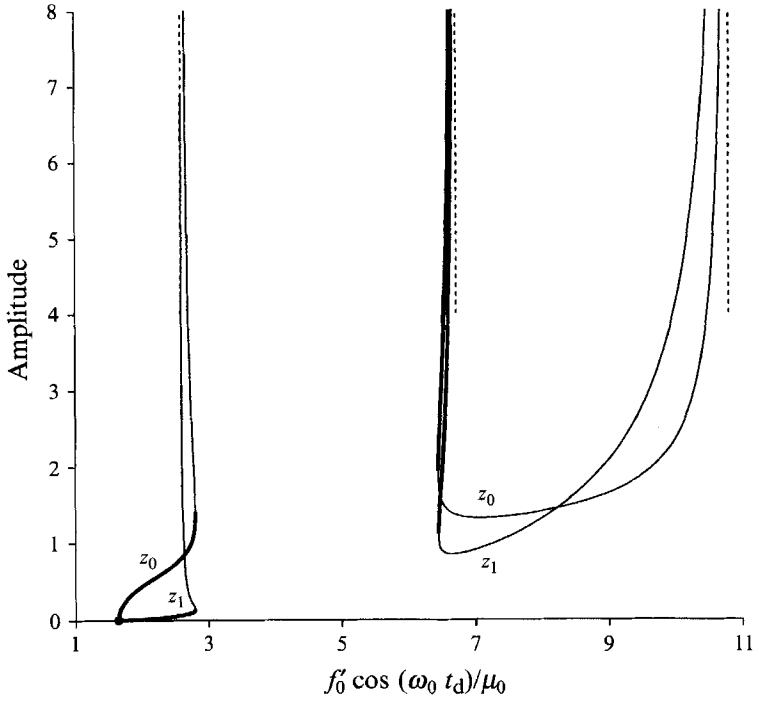

FIGURE 10. Same as figure 3 for larger values of $\mathscr{F}$. The (unphysical) large-amplitude branches do not satisfy the criteria for which a two-mode approximation is valid, and are spurious in the sense that they are not preserved using higher-order truncation schemes.

while figures 3, 6 and 7 compare different values of the viscosity μ_0, which, as mentioned earlier, is also the inverse Reynolds number of the basic unperturbed flow. Finally, figures 3, 8 and 9 compare different values of the time lag t_d between the third-order velocity and pressure at $z = 0$. In all of these results, we used the same values of the various parameters related to the particle loading ($\hat{\delta} = 0.5$, $\gamma_\pi = 5$, $\hat{L} = 0.5$, $\lambda = 0.5$ and $\hat{r}_0 = -1$, which gives $z_c^{(0)} = 0.5$). Qualitatively, the turning point occurs for larger values of f_0' (or $\mathscr{F}$) for both relatively large and small values of γ, which, as we recall, is the only parameter dependency of the nonlinear coefficients in the amplitude equations. Physically, the sound speed $\tilde{a}_0$ is proportional to the square root of this parameter, and we postulate that the effectiveness of the nonlinear coupling between growing and decaying modes is less for intermediate values of the acoustic wave speed that correspond to real gases, thereby resulting in larger amplitudes, and hence a smaller value of $\mathscr{F}_c$. Similarly, large values of the viscosity enhance damping, permitting larger amplitudes that result in smaller values of $\mathscr{F}_c$ (but larger values of the non-reduced coupling strength f_0'). Finally, a phase lag between the velocity and pressure oscillations at the entrance to the resonance tube allows a modest increase in the amplitudes of the acoustic oscillations, but permits a significant increase in the coupling strength before the turning point is reached. The latter, of course, reflects the fact that the effective coupling strength is greatly reduced (by an amount even larger than the factor $\cos(\omega_0 t_d)$ suggested by the linearized equations) when the pressure and velocity oscillations are not in phase.

The effects of particle loading in the present model are confined to the phase difference parameter λ_d, defined in terms of the imaginary parts of the linear growth rates according to (6.17). Consequently, the above remarks regarding the effects of the

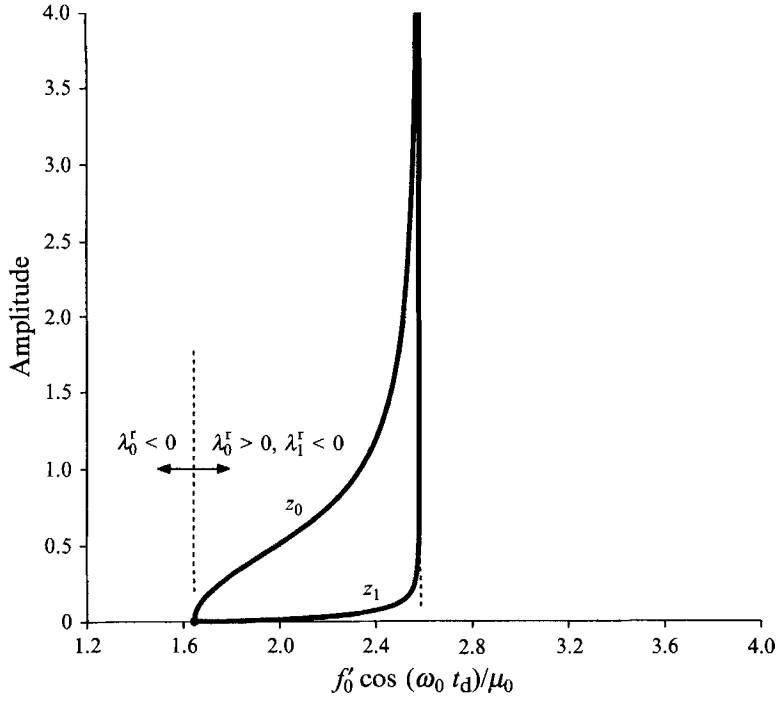

FIGURE 11. Same as figure 3 in the absence of particle loading ($\delta = 0$).

phase lag between the velocity and pressure oscillation apply to the effects of particle loading as well. In particular, particle loading, though neutral with respect to stability according to linear theory, is in fact a damping influence in the nonlinear regime. This can be readily seen by comparing figures 3 and 9 with figures 11 and 12, where the latter show the acoustic response in the absence of particle loading ($\delta = 0$) using the same remaining parameter values as in the earlier figures. In figure 11, the time lag t_d was also zero, resulting in $\lambda_d = 0$, and a consequent vanishing of the linear term in (6.28). As a result, the critical value $\mathscr{F}_c$ approaches a value $\hat{\mathscr{F}}_c$ determined by the vanishing of the coefficient of the quadratic term in that equation. Using the relations (6.18), this condition is given in terms of the real parts of the linear growth rates by

$$9(\lambda_0^r)^3 + 27(\lambda_0^r)^2 \lambda_1^r + 15\lambda_0^r(\lambda_1^r)^2 + (\lambda_1^r)^3 = 0, \tag{6.34}$$

independent of γ, and determines the location of the asymptote for the upper branch in figure 3 when λ_0^r and λ_1^r are expressed in terms of $\mathscr{F}$ according to (6.33). Thus, as particle loading decreases to zero, the turning point disappears, and the amplitudes become large (owing to the absence of any nonlinear phase damping). On the other hand, for the more realistic case of a non-zero phase difference between velocity and pressure at the entrance to the resonance tube (i.e. $t_d \neq 0$), the bend in the response does not vanish (since λ_d does not vanish) in the limit of zero particle loading. However, as a comparison of figures 9 and 12 shows, the value of $\mathscr{F}_c$ becomes smaller and the amplitude of the acoustic oscillations is larger when the total amount of phase damping due to the combination of coupling and particle loading is reduced. Thus, as is well known, the presence of particles can serve to dampen acoustic oscillations, even in the small-particle limit considered here. However, it should be noted that the damping mechanism described here is a nonlinear effect, distinct from the linear effects of drag that arise when the small-particle limit is relaxed (cf. Marble 1970).

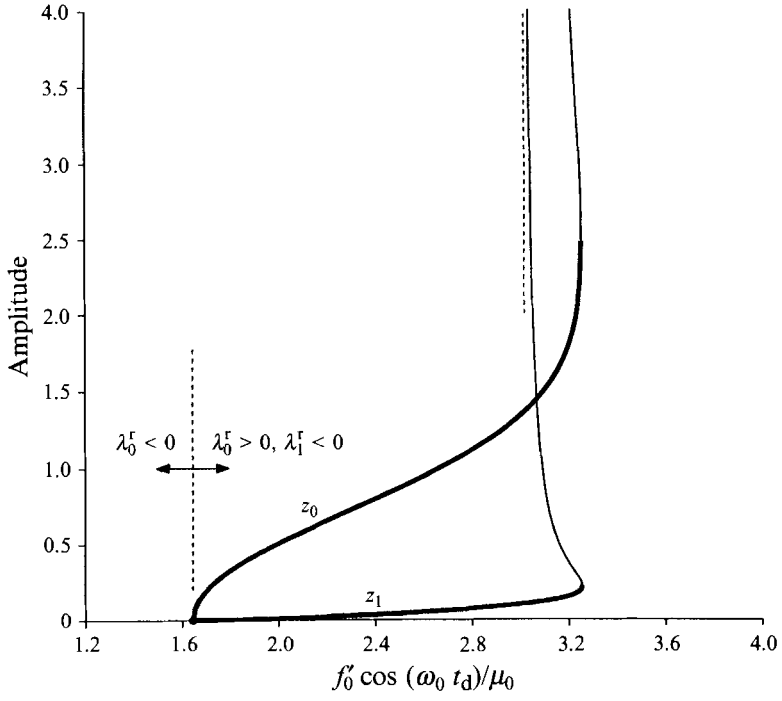

FIGURE 12. Same as figure 9 in the absence of particle loading ($\delta = 0$).

7. The three-mode approximation ($N' = 2$)

The fact that the turning point is achieved when the amplitude of the decaying mode is small compared with that of the growing mode is a strong indication that this aspect of the branching behaviour is physical. Nonetheless, it is of interest to quantitatively compare the two-mode results with those obtained when three modes are retained. Indeed, it is expected that there will be some shift to the right in the location of the turning point when additional decaying modes are retained, since the presence of these additional modes should enhance the process whereby energy is transferred from the growing mode and dissipated. Thus, from (4.27), the three-mode approximation is, after introducing real amplitudes $R_l(\tau)$ and phases $\phi_l(\tau)$ as before,

$$\frac{dR_0}{d\tau} = \lambda_0^r R_0 - \lambda^i_{\bar{0},\bar{0},1} R_0^2 R_1 \sin\psi - \lambda^i_{1,1,\bar{2}} R_1^2 R_2 \sin\hat{\psi} - \lambda^i_{\bar{0},\bar{1},2} R_0 R_1 R_2 \sin(\psi - \hat{\psi}), \tag{7.1}$$

$$\frac{dR_1}{d\tau} = \lambda_1^r R_1 + \lambda^i_{0,0,0} R_0^3 \sin\psi + \lambda^i_{0,\bar{1},2} R_0 R_1 R_2 \sin\hat{\psi} - \lambda^i_{\bar{0},\bar{0},2} R_0^2 R_2 \sin(\psi - \hat{\psi}), \tag{7.2}$$

$$\frac{dR_2}{d\tau} = \lambda_2^r R_2 - \lambda^i_{\bar{0},1,1} R_0 R_1^2 \sin\hat{\psi} + \lambda^i_{0,0,1} R_0^2 R_1 \sin(\psi - \hat{\psi}), \tag{7.3}$$

$$\frac{d\psi}{d\tau} = \lambda_a + \lambda_p R_0^2 + \lambda_q R_1^2 + \lambda_r R_2^2 + (\lambda^i_{0,0,0} R_0^3 R_1^{-1} - 3\lambda^i_{\bar{0},\bar{0},1} R_0 R_1)\cos\psi$$
$$+ (\lambda^i_{0,\bar{1},2} R_0 R_2 - 3\lambda^i_{1,1,\bar{2}} R_0^{-1} R_1^2 R_2)\cos\hat{\psi} + (\lambda^i_{\bar{0},\bar{0},2} R_0^2 R_1^{-1} R_2 - 3\lambda^i_{\bar{0},\bar{1},2} R_1 R_2)\cos(\psi - \hat{\psi}), \tag{7.4}$$

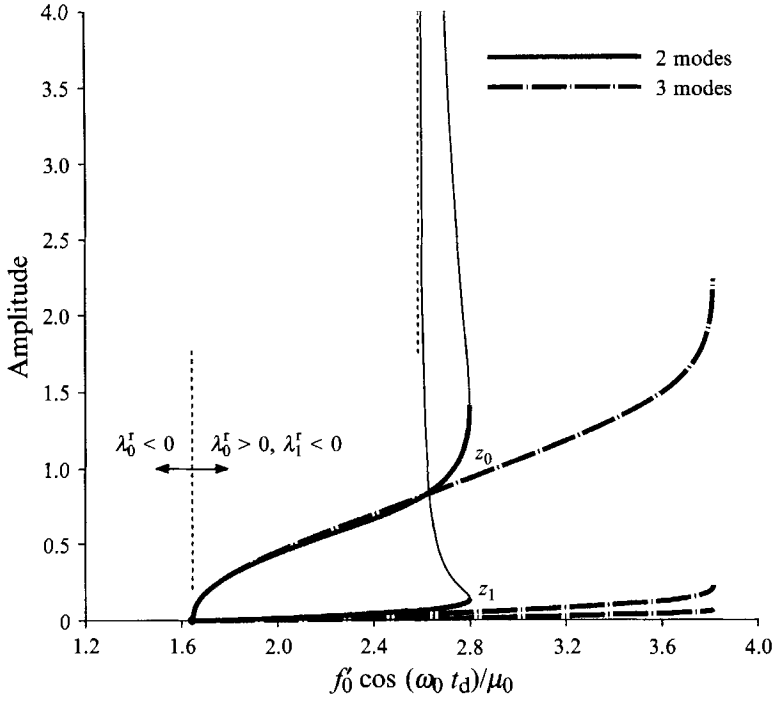

FIGURE 13. Comparison of the two-mode and three-mode approximations for the parameter values used in figure 3.

$$\frac{\mathrm{d}\hat{\psi}}{\mathrm{d}\tau} = \rho_d + \rho_p R_0^2 + \rho_q R_1^2 + \rho_r R_2^2 + (2\lambda^{\mathrm{i}}_{0,0,0} R_0^3 R_1^{-1} - \lambda^{\mathrm{i}}_{\bar{0},\bar{0},1} R_0 R_1)\cos\psi$$
$$+ (2\lambda^{\mathrm{i}}_{0,\bar{1},2} R_0 R_2 - \lambda^{\mathrm{i}}_{1,1,\bar{2}} R_0^{-1} R_1^2 R_2 - \lambda^{\mathrm{i}}_{\bar{0},1,1} R_0 R_1^2 R_2^{-1})\cos\hat{\psi}$$
$$+ (2\lambda^{\mathrm{i}}_{\bar{0},\bar{0},2} R_0^2 R_1^{-1} R_2 - \lambda^{\mathrm{i}}_{\bar{0},\bar{1},2} R_1 R_2 - \lambda^{\mathrm{i}}_{0,0,1} R_0^2 R_1 R_2^{-1})\cos(\psi - \hat{\psi}), \quad (7.5)$$

where, in addition to the relative phase $\psi \equiv \phi_1 - 3\phi_0$ introduced in connection with the two-mode approximation, we have introduced the additional phase difference variable $\hat{\psi} = 2\phi_1 - \phi_0 - \phi_2$. In addition to the coefficients defined in (6.4)–(6.9) in connection with the two-mode case, the other coefficients that now enter into the analysis are defined by (6.4) and (6.5) for $l = 2$, (6.7) for $l = 1$, (6.8) and (6.9) for $l \leqslant 1$, $l' = 1$, and by

$$\lambda_{0,0,1} = \mathrm{i}\lambda^{\mathrm{i}}_{0,0,1} = \zeta_0(\omega_2, \omega_0, \omega_0, \omega_1) + \zeta_0(\omega_2, \omega_0, \omega_1, \omega_0) + \zeta_0(\omega_2, \omega_1, \omega_0, \omega_0), \quad (7.6)$$
$$\lambda_{1,1,\bar{2}} = \mathrm{i}\lambda^{\mathrm{i}}_{1,1,\bar{2}} = \zeta_1(\omega_0, \omega_1, \omega_1, \omega_2) + \eta_1(\omega_0, \omega_2, \omega_1, \omega_1) + \xi_1(\omega_0, \omega_1, \omega_2, \omega_1), \quad (7.7)$$
$$\lambda_{\bar{0},1,1} = \mathrm{i}\lambda^{\mathrm{i}}_{\bar{0},1,1} = \zeta_1(\omega_2, \omega_1, \omega_1, \omega_0) + \eta_1(\omega_2, \omega_0, \omega_1, \omega_1) + \xi_1(\omega_2, \omega_1, \omega_0, \omega_1), \quad (7.8)$$
$$\lambda_{0,\bar{1},2} = \mathrm{i}\lambda^{\mathrm{i}}_{0,\bar{1},2} = \zeta_1(\omega_1, \omega_0, \omega_2, \omega_1) + \zeta_1(\omega_1, \omega_2, \omega_0, \omega_1) + \eta_1(\omega_1, \omega_1, \omega_0, \omega_2)$$
$$+ \eta_1(\omega_1, \omega_1, \omega_2, \omega_0) + \xi_1(\omega_1, \omega_0, \omega_1, \omega_2) + \xi_1(\omega_1, \omega_2, \omega_1, \omega_0), \quad (7.9)$$
$$\lambda_{\bar{0},\bar{1},2} = \mathrm{i}\lambda^{\mathrm{i}}_{\bar{0},\bar{1},2} = \zeta_2(\omega_0, \omega_0, \omega_1, \omega_2) + \zeta_2(\omega_0, \omega_1, \omega_0, \omega_2) + \eta_2(\omega_0, \omega_2, \omega_0, \omega_1)$$
$$+ \eta_2(\omega_0, \omega_2, \omega_1, \omega_0) + \xi_2(\omega_0, \omega_0, \omega_2, \omega_1) + \xi_2(\omega_0, \omega_1, \omega_2, \omega_0), \quad (7.10)$$

and

$$\rho_d \equiv 2\lambda^{\mathrm{i}}_1 - \lambda^{\mathrm{i}}_0 - \lambda^{\mathrm{i}}_2, \quad \rho_p \equiv 2\lambda^{\mathrm{i}}_{0,\bar{0},1} - \lambda^{\mathrm{i}}_{0,0,\bar{0}} - \lambda^{\mathrm{i}}_{0,\bar{0},2}, \quad \rho_q \equiv 2\lambda^{\mathrm{i}}_{1,1,\bar{1}} - \lambda^{\mathrm{i}}_{0,1,\bar{1}} - \lambda^{\mathrm{i}}_{1,\bar{1},2}, \quad (7.11)$$

$$\lambda_r \equiv \lambda^{\mathrm{i}}_{1,2,\bar{2}} - 3\lambda^{\mathrm{i}}_{0,2,\bar{2}}, \quad \rho_r \equiv 2\lambda^{\mathrm{i}}_{1,2,\bar{2}} - \lambda^{\mathrm{i}}_{0,2,\bar{2}} - \lambda^{\mathrm{i}}_{2,2,\bar{2}}. \quad (7.12)$$

In comparing (7.1)–(7.5) with (6.14)–(6.16), we see that the latter are recovered from the former when R_2 is set to zero. Thus, we anticipate that the three-mode approximation will give a refinement of the results found in the two-mode analysis, and figure 13, in which the curve corresponding to three modes was obtained by long-time numerical integration of (7.1)–(7.5) from initial conditions, shows that this expectation is indeed realized. In particular, the two-mode approximation is quite accurate except as the turning point $\mathscr{F} = \mathscr{F}_c$ is approached, where a correction in its location is evident. However, we note that the revised location of the turning point still occurs far below the value (in this particular example) $\mathscr{F}_1 = \frac{2}{3}\omega_1^2 = 9\mathscr{F}_0$, where the second mode becomes linearly unstable, and even further from the value $\mathscr{F}_2 = \frac{2}{3}\omega_2^2 = 25\mathscr{F}_0$ where the third mode loses linear stability. In addition, at the turning point, it is still true that the ratios z_1/z_0 and z_2/z_1 (where $z_l = R_l^2$) are both small, which again supports the notion that the turning point is physical, and not a consequence of truncation. Of course, the inclusion of an additional decaying mode supports quantitatively larger values of $\mathscr{F}$ and larger amplitudes at the turning point since the system is able to transfer and dissipate more energy from the growing mode via the various additional coupling terms in (7.1)–(7.5). However, the conclusion here is that, as a general rule, this mechanism becomes less efficient the larger the frequency separation between a growing and a decaying mode. That is, the inclusion of one decaying mode was essential to obtaining physical results, but the inclusion of a second decaying mode had only a quantitative, as opposed to qualitative, effect on the results in this regime. Consequently, we conjecture, based on the above analysis with two and three modes, that a convergence in the value $\mathscr{F}_c$ would be realized as additional modes are retained in the truncation scheme. Of course, further calculations with larger numbers of modes would be valuable here, providing greater insight into the effects of mode truncation on the bifurcation structure associated with acoustic instability.

As mentioned earlier, additional branches for which z_1/z_0 was no longer small (figure 10) were obtained for significantly larger values of $\mathscr{F} < \mathscr{F}_1$ using the two-mode approximation. These, however, appear to be an artifact of the truncation and (the stable portions, at least) were not reproducible using the three-mode approximation (7.1)–(7.5). Indeed, in that parameter regime, only unbounded solutions of (7.1)–(7.5) were obtained.

8. Conclusions

The present work has shown how the equations governing acoustic oscillations in partially enclosed volumes can be formally reduced to a system of ordinary evolution equations for the amplitudes of linear acoustic modes. The success of this procedure depends on first appropriately scaling the magnitude of acoustic perturbations relative to the basic steady flow variables, and then applying a nonlinear stability analysis to obtain solvability conditions for the existence of non-trivial solutions at each order. In the present problem, it is necessary, owing to the open boundary conditions at the end of the tube, to carry out the perturbation analysis to third order to obtain the necessary conditions on the leading-order amplitudes. In other related problems, such as combustion instabilities in rocket motors discussed in §1, the commonly used closed-boundary conditions result in non-trivial solvability conditions at the second order. Consequently, the types of nonlinearities (cubic in the former, quadratic in the latter) that appear in the resulting amplitude equations depend strongly on the nature of the boundary conditions that are applied. This may be particularly significant for the rocket motor stability problem, for which the closed exit condition is clearly an

approximation. In particular, a modification in this condition to model more accurately the actual physical situation may lead to amplitude equations for the modified eigenfunctions that support qualitatively different dynamics.

Another feature of the present analysis is that, unlike those problems for which a dispersion relation leading to a neutral stability boundary is obtained from a linearized analysis, linear stability theory (equations (3.1)) predicts the presence of all acoustic modes ((3.2)–(3.5), (4.1)–(4.3)), giving no information on growth rates. This is due to the fact that the linearized problem is homogeneous since the inhomogeneous coupling between the combustion chamber and the resonance tube, as represented by the boundary condition at $z = 0$, does not enter into the analysis until $O(\epsilon^3)$. Consequently, the growth rates corresponding to these eigenfunctions are only obtained at correspondingly higher orders in the perturbation analysis. Since all acoustic modes appear at leading order, the solvability conditions thus lead to an infinitely-coupled system of amplitude equations (equations (3.11) and (4.27)), rather than the finite type of system that typically arises from the nonlinear stability of discrete modes in the neighbourhood of a neutral stability boundary of the linearized problem (cf. Margolis & Matkowsky 1985; Booty, Margolis & Matkowsky 1987; Margolis 1991*a*, *b*; Bechtold & Margolis 1991).

Based on a knowledge of the growth rates corresponding to the linearized amplitude equations, it is reasonable to expect that an appropriately truncated version of the infinite system can provide a valid approximation under certain conditions. Some guidelines for truncating the system were thus presented, and illustrated with a complete analysis of limit cycle behaviour for the case of two longitudinal modes. A comparison with numerical results obtained for a three-mode truncation then provided additional evidence of the validity of a two- or three-mode analysis in the common case when only the first mode has a positive growth rate. We remark, however, that when two or more modes have positive linear growth rates, it can be anticipated that higher-order truncation schemes may be required owing to natural resonances that may occur between different modes that are separated on the eigenfrequency spectrum (Margolis 1993). In addition, for some types of problems (such as that due to the forced motion of a piston), the presence of shocks or steep waves can require the retention of many modes in order to provide sufficient modal resolution (cf. Wang & Kassoy 1990*a*–*c*).

The general result based on our two- and three-mode analyses was the stable bifurcation of a limit cycle corresponding to a steady-amplitude acoustic oscillation at a critical value of a parameter that reflects the strength of the coupling of the resonance tube to its combustion source. Thus, the present model succeeds in capturing the basic phenomenon behind the operation of actual pulse combustors. Ultimately, the bifurcation branch reaches a turning point which, we conjecture, could be qualitatively preserved under still further modal resolution. Beyond this point our model predicts no steady limit-cycle behaviour. Indeed, numerical calculations in this regime lead to unbounded growth of the amplitudes, suggesting that additional damping mechanisms and/or a rescaling to accommodate large amplitudes would be required to describe bounded solutions there.

Finally, we emphasize that a relatively simple physical model was chosen in this work primarily to illustrate a general approach to analysing nonlinear acoustic behaviour by strictly formal methods. Based on our two-mode analysis and our preliminary calculations with three modes, steady limit-cycle behaviour was the only non-trivial acoustic behaviour predicted, at least for the case in which only the first mode is linearly unstable. Although this is in qualitative agreement with both experiments (cf. Dec & Keller 1990; Dec *et al.* 1991) and direct numerical calculations

(cf. Barr *et al.* 1988, 1990), it seems likely, based on the general structure of the dynamical system of amplitude evolution equations derived here, that non-periodic acoustic oscillations arising from additional bifurcations are possible in these systems. Consequently, in future work we plan to analyse more detailed physical models and to study higher-order truncation schemes for cases in which two or more modes may have positive growth rates. We anticipate that either or both extensions of the present work will then lead to more complex dynamical solutions of the corresponding amplitude equations.

This work was supported by the Applied Mathematical Sciences Research Program, Office of Energy Research, US Department of Energy.

Appendix A. Solvability conditions

In order for solutions to the nth-order problem (3.7) to exist, it is necessary that the inhomogeneous terms satisfy the solvability conditions (3.8) for any solution $\not{p}^\dagger, \boldsymbol{v}^\dagger$ satisfying the adjoint of the homogeneous problem (3.1). To derive both the adjoint problem and these conditions, it is convenient to write (3.7a, b) in the vector form

$$\mathscr{L}\begin{Bmatrix} \not{p}_n \\ u_n \\ v_n \\ w_n \end{Bmatrix} \equiv \begin{bmatrix} \partial/\partial t & \partial/\partial x & \partial/\partial y & \partial/\partial z \\ \partial/\partial x & \partial/\partial t & 0 & 0 \\ \partial/\partial y & 0 & \partial/\partial t & 0 \\ \partial/\partial z & 0 & 0 & \partial/\partial t \end{bmatrix}\begin{Bmatrix} \not{p}_n \\ u_n \\ v_n \\ w_n \end{Bmatrix} = \begin{Bmatrix} q_n \\ r_{1,n} \\ r_{2,n} \\ r_{3,n} \end{Bmatrix}, \tag{A 1}$$

where (u_n, v_n, w_n) are the x-, y- and z-components of the velocity vector $\boldsymbol{v}$. We now introduce, for any two complex vectors $\boldsymbol{a}$ and $\boldsymbol{b}$, the inner products

$$\langle \boldsymbol{a}, \boldsymbol{b} \rangle = \lim_{T\to\infty} \frac{1}{abT} \int_0^T \mathrm{d}t \int_0^a \mathrm{d}x \int_0^b \mathrm{d}y \int_0^1 \mathrm{d}z (\boldsymbol{a}\cdot\boldsymbol{b}^*), \tag{A 2}$$

$$(\boldsymbol{a}, \boldsymbol{b}) = \lim_{T\to\infty} \frac{1}{abT} \int_0^T \mathrm{d}t \int_0^a \mathrm{d}x \int_0^b \mathrm{d}y (\boldsymbol{a}\cdot\boldsymbol{b}^*), \tag{A 3}$$

$$[\boldsymbol{a}, \boldsymbol{b}] = \lim_{T\to\infty} \frac{1}{abT} \int_0^T \mathrm{d}t \int_0^b \mathrm{d}y \int_0^1 \mathrm{d}z (\boldsymbol{a}\cdot\boldsymbol{b}^*), \tag{A 4}$$

$$\{\boldsymbol{a}, \boldsymbol{b}\} = \lim_{T\to\infty} \frac{1}{abT} \int_0^T \mathrm{d}t \int_0^a \mathrm{d}x \int_0^1 \mathrm{d}z (\boldsymbol{a}\cdot\boldsymbol{b}^*), \tag{A 5}$$

$$|\boldsymbol{a}, \boldsymbol{b}| = \lim_{T\to\infty} \frac{1}{abT} \int_0^a \mathrm{d}x \int_0^b \mathrm{d}y \int_0^1 \mathrm{d}z (\boldsymbol{a}\cdot\boldsymbol{b}^*), \tag{A 6}$$

where the asterisk denotes the complex conjugate. Then, by routine operations, we obtain the identity

$$\left\langle \begin{Bmatrix} \not{p}_n^\dagger \\ u_n^\dagger \\ v_n^\dagger \\ w_n^\dagger \end{Bmatrix}, \mathscr{L}\begin{Bmatrix} \not{p}_n \\ u_n \\ v_n \\ w_n \end{Bmatrix} \right\rangle = \left[\begin{Bmatrix} \not{p}_n^\dagger \\ u_n^\dagger \\ v_n^\dagger \\ w_n^\dagger \end{Bmatrix}, \begin{Bmatrix} \not{p}_n \\ u_n \\ v_n \\ w_n \end{Bmatrix} \right]\Bigg|_{t=0}^{T} + \left[\left[\begin{Bmatrix} u_n^\dagger \\ \not{p}_n^\dagger \\ 0 \\ 0 \end{Bmatrix}, \begin{Bmatrix} \not{p}_n \\ u_n \\ 0 \\ 0 \end{Bmatrix} \right] \right]\Bigg|_{x=0}^{a}$$

$$+ \left\{ \begin{Bmatrix} v_n^\dagger \\ 0 \\ \not{p}_n^\dagger \\ 0 \end{Bmatrix}, \begin{Bmatrix} \not{p}_n \\ 0 \\ v_n \\ 0 \end{Bmatrix} \right\}\Bigg|_{y=0}^{b} + \left(\begin{Bmatrix} w_n^\dagger \\ 0 \\ 0 \\ \not{p}_n^\dagger \end{Bmatrix}, \begin{Bmatrix} \not{p}_n \\ 0 \\ 0 \\ w_n \end{Bmatrix} \right)\Bigg|_{z=0}^{1} - \left\langle \mathscr{L}\begin{Bmatrix} \not{p}_n^\dagger \\ u_n^\dagger \\ v_n^\dagger \\ w_n^\dagger \end{Bmatrix}, \begin{Bmatrix} \not{p}_n \\ u_n \\ v_n \\ w_n \end{Bmatrix} \right\rangle. \tag{A 7}$$

Requiring that this identity be satisfied for the homogeneous case $n = 1$ implies that the left-hand side vanishes, giving the condition that the right-hand side vanish as well. Consequently, the latter is satisfied if the adjoint solution $\not{p}^\dagger, \boldsymbol{v}^\dagger$ is any (bounded) solution of the homogeneous problem (3.1), which is therefore self-adjoint. Using this result and (A 1), equation (A 7) collapses to

$$\left\langle \begin{Bmatrix} \not{p}_n^\dagger \\ u_n^\dagger \\ v_n^\dagger \\ w_n^\dagger \end{Bmatrix}, \begin{Bmatrix} q_n \\ r_{1,n} \\ r_{2,n} \\ r_{3,n} \end{Bmatrix} \right\rangle + \left(\begin{Bmatrix} 0 \\ 0 \\ 0 \\ \not{p}_n^\dagger|_{z=0} \end{Bmatrix}, \begin{Bmatrix} 0 \\ 0 \\ 0 \\ b_n \end{Bmatrix} \right) = 0, \tag{A 8}$$

which, for the case of purely longitudinal modes, is equivalent to (3.8).

Appendix B. Boundary effects

In the presentation of the model in §2.1, explicit consideration of sidewall effects and possible 'radiation damping' out the end of the resonance tube was suppressed in favour of a volumetric damping term. However, as suggested by a reviewer, an explicit consideration of boundary and radiation damping may be readily incorporated into the analysis by specifying admittance/impedance types of boundary conditions at the sidewalls and at the end of the resonance tube. These may be written in a generalized form similar to that used to relate velocity and pressure at the entrance to the resonance tube (equation 2.6*c*)). In particular, the boundary condition (2.6*a*) at $z = \tilde{H}$ may be replaced by the relation

$$\tilde{p}|_{\tilde{z}=\tilde{H}} = \tilde{g}(\tilde{u}_z(\tilde{t}-\tilde{t}_e)), \quad \tilde{g}(\tilde{w}_0) = \tilde{p}_0, \tag{B 1}$$

where $\tilde{u}_z = \boldsymbol{n}_z \cdot \tilde{\boldsymbol{u}}$ is the velocity component in the $+\tilde{z}$-direction. In non-dimensional form, this leads to a leading-order relation for the time-dependent pressure perturbation $\not{p}$ at $z = 1$ given by $\not{p} = M^2 g_0' w|_{z=1,\, t=t-t_e}$, where w is the time-dependent perturbation component of longitudinal velocity, and $g_0' = (\tilde{a}_0/\tilde{\rho}_0 \tilde{w}_0^2)(\mathrm{d}\tilde{g}/\mathrm{d}\tilde{u}_z)|_{\tilde{w}_0}$. Thus, based on this scaling, $O(1)$ values of the non-dimensional impedance coefficient g_0' will result in an $O(\epsilon M^2) \sim O(\epsilon^5)$ pressure perturbation at $z = 1$. However, if we formally consider values of this coefficient which are $O(1/M)$ by introducing $\hat{g}_0' = Mg_0'$, then the contribution appears at $O(\epsilon^3)$, so that in (3.7), $\not{p}_1|_{z=1} = \not{p}_2|_{z=1} = 0$, but $\not{p}_3|_{z=1} = \hat{M}\hat{g}_0' w_1|_{z=1,\, t=t-t_e}$. This inhomogeneous term than contributes to the solvability condition (A 7) at this order, which, for the case of purely longitudinal modes, results in an additional linear term $\alpha_l^e MA_l$ on the right-hand side of the amplitude equations (3.11), where

$$\alpha_l^e = -\hat{g}_0' \exp(-\mathrm{i}\omega_l t_e). \tag{B 2}$$

Thus, the linear growth rate of the lth longitudinal mode given previously by (3.12) contains the additional contribution Δ_l^e given by

$$\Delta_l^e = -M\hat{g}_0' \cos(\omega_l t_e). \tag{B 3}$$

This calculation thus shows that although radiation damping introduces additional parameter and modal frequency dependencies into the expression for the linear growth rate of each acoustic mode, it introduces no change in the form of the amplitude equations themselves or in the expressions for the coefficients of the nonlinear terms in those equations. Consequently, a supercritical acoustic bifurcation is still predicted at a critical value of the driving parameter f_0'' at which the expression for the linear growth rate first vanishes for some particular mode.

A similar calculation can be performed with respect to the sidewalls as well. In particular, if we interpret these boundaries as the edge of the acoustic boundary layer, then we may relax (2.6*b*) to admit a normal velocity perturbation that is coupled to the local pressure perturbation. Thus, we now replace (2.6*c*) with an admittance condition

$$\boldsymbol{n}\cdot\tilde{\boldsymbol{u}}|_C = \tilde{h}(\tilde{p}(\tilde{t}-\tilde{t}_s)), \quad \tilde{h}(\tilde{p}_0) = 0, \tag{B 4}$$

where $\boldsymbol{n}$ denotes the outward normal on any side boundary C. This is the same type of condition as (2.6*c*), and consequently, the third-order solvability conditions (A 7) lead to the additional linear term $\alpha_l^s MA_l$ on the right-hand side of the amplitude equations (3.11), where

$$\alpha_l^s = -4h_0' \exp(-i\omega_l t_s), \tag{B 5}$$

and the admittance coefficient $h_0' = (\tilde{\rho}_0 \tilde{a}_0^2/\tilde{w}_0)(d\tilde{h}/d\tilde{p}|_{\tilde{p}_0}) \sim O(1)$. This in turn contributes an additional term Δ_l^s given by

$$\Delta_l^s = -4Mh_0' \cos(\omega_l t_s) \tag{B 6}$$

to the linear growth rate of the lth longitudinal mode. Consequently, the form of the amplitude equations and the coefficients of the nonlinear terms in those equations are again unchanged, thereby preserving the nature of the acoustic bifurcation described in the main body of the paper.

REFERENCES

Barr, P. K., Dwyer, H. A. & Bramlette, T. T. 1988 A one-dimensional model of a pulse combustor. *Combust. Sci. Tech.* **58**, 315–336.

Barr, P. K., Keller, J. O., Bramlette, T. T., Westbrook, C. K. & Dec, J. E. 1990 Pulse combustor modeling: demonstration of the importance of characteristic times. *Combust. Flame* **82**, 252–269.

Bechtold, J. K. & Margolis, S. B. 1989 Hydrodynamic stability of solid and liquid propellant combustion. *Combust. Sci. Tech.* **68**, 49–84.

Bechtold, J. K. & Margolis, S. B. 1991 Nonlinear hydrodynamic stability and spinning deflagration of liquid propellants. *SIAM J. Appl. Maths* **51**, 1356–1379.

Booty, M. R., Margolis, S. B. & Matkowsky, B. J. 1987 Interaction of pulsating and spinning waves in nonadiabatic flame propagation. *SIAM J. Appl. Maths* **47**, 1241–1286.

Bramlette, T. T. & Keller, J. O. 1987 Theoretical and experimental investigation of a new pulse combustor. *Sandia National Laboratories Rep.* 86-8050.

Constantin, P., Foias, C., Manley, O. P. & Temam, R. 1985 Determining modes and fractal dimension of turbulent flows. *J. Fluid Mech.* **150**, 427–440.

Culick, F. E. C. 1976*a* Nonlinear behavior of acoustic waves in combustion chambers – I. *Acta Astron.* **3**, 715–734.

Culick, F. E. C. 1976*b* Nonlinear behavior of acoustic waves in combustion chambers – II. *Acta Astron.* **3**, 735–757.

Culick, F. E. C. 1993 Some recent results for nonlinear acoustics in combustion chambers. *AIAA Paper* 90-3927 and *AIAA J.* (to appear).

Culick, F. E. C. & Yang, V. 1992 Prediction of the stability of unsteady motions in solid propellant rocket motors. In *Nonsteady Burning and Combustion Stability of Solid Propellants* (ed. L. DeLuca & M. Summerfield). AIAA (Progress in Astronautics and Aeronautics, vol. 143, pp. 719–779).

Dec, J. E. & Keller, J. O. 1990 Time-resolved gas temperatures in the oscillating turbulent flow of a pulse combustor tail pipe. *Combust. Flame* **80**, 358–370.

Dec, J. E., Keller, J. O. & Hongo, I. 1991 Time-resolved velocities and turbulence in the oscillating flow of a pulse combustor tail pipe. *Combust. Flame* **83**, 271–292.

Foias, C., Jolly, M. S., Kevrekidis, I. G., Sell, G. R. & Titi, E. S. 1988 On the computation of inertial manifolds. *Phys. Lett.* A **131**, 433–436.

FOIAS, C. & TRÈVE, Y. M. 1981 Minimum number of modes for the approximation of the solutions of the Navier–Stokes equations in two and three dimensions. *Phys. Lett.* A **85**, 35–37.

GRAD, H. 1949 Resonance burning in rocket motors. *Commun. Pure Appl. Maths* **2**, 79–102.

INGRAHAM, R. L. 1990 A sequence of Galerkin approximations to the center manifold for a certain class of nonlinear partial differential equational dynamical systems. *SIAM J. Appl. Maths* **50**, 956–971.

LAW, C. K. 1982 Recent advances in droplet vaporization and combustion. *Prog. Energy Combust. Sci.* **8**, 171–199.

MANLEY, O. P. & TRÈVE, Y. M. 1981 Minimum number of modes in approximate solutions to equations of hydrodynamics. *Phys. Lett.* A **82**, 88–90.

MARBLE, F. E. 1970 Dynamics of dusty gases. In *Ann. Rev. Fluid Mech.* **2**, 397–446.

MARGOLIS, S. B. 1991*a* The transition to nonsteady deflagration in gasless combustion. *Prog. Energy Combust. Sci.* **71**, 135–162.

MARGOLIS, S. B. 1991*b* Chaotic combustion of solids and high-density fluids near points of strong resonance. *Proc. R. Soc. Lond.* A **433**, 131–150.

MARGOLIS, S. B. 1992 Stability of acoustic oscillations in a model Helmholtz-type pulse combustor. *Twenty-Fourth Symp. (Intl) on Combustion*, pp. 19–27.

MARGOLIS, S. B. 1993 Resonant mode interactions and the bifurcation of combustion-driven acoustic oscillations in resonance tubes. (To appear.)

MARGOLIS, S. B. & MATKOWSKY, B. J. 1983 Nonlinear stability and bifurcation in the transition from laminar to turbulent flame propagation. *Combust. Sci. Tech.* **34**, 45–77.

MARGOLIS, S. B. & MATKOWSKY, B. J. 1985 Flame propagation in channels: secondary bifurcation to quasi-periodic pulsations. *SIAM J. Appl. Maths* **45**, 93–129.

MARGOLIS, S. B. & WILLIAMS, F. A. 1988 Diffusional/thermal coupling and intrinsic instability of solid propellant combustion. *Combust. Sci. Tech.* **59**, 27–84.

MARGOLIS, S. B. & WILLIAMS, F. A. 1989 Diffusional/thermal instability of a solid propellant flame. *SIAM J. Appl. Maths* **49**, 1390–1420.

MATKOWSKY, B. J. 1970 Nonlinear dynamic stability: a formal theory. *SIAM J. Appl. Maths* **18**, 872–883.

PAPARIZOS, L. G. & CULICK, F. E. C. 1989 The two-mode approximation to nonlinear acoustics in combustion chambers – I. Exact solution for second order acoustics. *Combust. Sci. Tech.* **65**, 39–65.

PRAKASH, S. & SIRIGNANO, W. A. 1980 Theory of convective droplet vaporization with unsteady heat transfer in the circulating liquid phase. *Intl J. Heat Mass Transfer* **23**, 253–268.

PUTNAM, A. A., BELLES, F. E. & KENTFIELD, J. A. C. 1986 Pulse combustion. *Prog. Energy Combust. Sci.* **12**, 43–79.

RAYLEIGH, J. W. S. 1878 The nature of certain acoustical phenomena. *Nature* **18**, 319.

SUMMERFIELD, M. 1951 A theory of unstable propulsion in liquid propellant rocket systems. *ARS J.* **21**, 108–114.

TEMKIN, S. 1981 *Elements of Acoustics*. Wiley.

TRÈVE, Y. M. 1981 Number of modes controlling fluid flows from experimentally measurable quantities. *Phys. Lett.* A **85**, 81–83.

WANG, M. & KASSOY, D. R. 1990*a* Dynamic response of an inert gas to slow piston acceleration. *J. Acoust. Soc. Am.* **87**, 1466–1471.

WANG, M. & KASSOY, D. R. 1990*b* Dynamic compression and weak shock formation in an inert gas due to fast piston acceleration. *J. Fluid Mech.* **220**, 267–292.

WANG, M. & KASSOY, D. R. 1990*c* Evolution of weakly nonlinear waves in a cylinder with a movable piston. *J. Fluid Mech.* **221**, 23–52.

WILLIAMS, F. A. 1985 *Combustion Theory*. Benjamin/Cummings.

YANG, V. & CULICK, F. E. C. 1990 On the existence and stability of limit cycles for transverse acoustic oscillations in a cylindrical combustion chamber. *Combust. Sci. Tech.* **72**, 37–65.

ZINN, B. T. & POWELL, E. A. 1971 Nonlinear combustion stability in liquid-propellant rocket engines. *Thirteenth Symp. (Intl) on Combustion*, pp. 491–503.